1. **Contract Number: C46-41-01**

2. A predictive model of the $^{40}Ar/^{39}Ar$ age dating system in Faroe Islands basalts to assist in well sampling and the positioning of sidewall core in future offshore drilling projects

3. Dr Sarah C Sherlock[1] Dr David W Jolley[2]
Professor Simon P Kelley[1] Dr Jonathon Watson[3]

4. [1]Department of Earth and Environmental Sciences, The Open University, Walton Hall, Milton Keynes, United Kingdom.
[2]Department of Geology and Petroleum Geology, University of Aberdeen, King's College, Meston Building, Aberdeen, United Kingdom.
[3]Planetary and Space Sciences Research Institute, The Open University, Walton Hall, Milton Keynes, United Kingdom.

5. 31st March 2011

6. b. Regional geology and the evolution of the entire Faroese area.

7. Budget received so far: 547,813 DKK Total cost of project: 1,416,397 DKK

8. Start date of contract: 1st July 2008 End date of contract: 30th June 2010

9. Date of final report: 31st July 2010

10. Abstract

A detailed study of Ar/Ar age and environmental deposition of lavas in the NAIP, namely Mull and the Faroes Islands, identifies that the Ar/Ar age within a lava is strongly determined by the cooling rate of the lava, and the presence of standing water during emplacement. During the study the sampling and preparation techniques for Ar/Ar dating have been refined such that dating basalts by Ar/Ar is more cost efficient than previously. The bases of the lavas are the most appropriate target for sampling for Ar/Ar dating and lavas in contact with water-lain sediments are most likely to yield an accurate age. Lavas from Mull and the Faroes Islands (Malinstindur and Enni Formations) are within error of 55 Ma inkeeping with the palynological data and younger than the previously-published Ar/Ar ages.

11. Introduction

Conventional sampling for Ar/Ar dating dictates that a single sample is collected from the seemingly freshest part of a lava, with the assessment of 'freshness' taken in the field/core store. Our strategy to sample at a much higher resolution shows that this is not appropriate and that the most rapidly-cooled part of a lava is most likely to yield accurate Ar/Ar age information.

The following statement occurs in section 11 of C46-41-01 interim report (1st June 2009):

"Ultimately, vesiculated fine-grained unweathered basalt from the 'core' of a lava would be the most appropriate for Ar/Ar dating but these are infrequent in the North Atlantic Igneous

Province. We anticipate that we will see adverse affects at the base and top of the lava and next have to address the question of how pervasive these are, with the forthcoming Ar/Ar datasets. Based on current observations we would sample at between 30% and 40% the height of the lava from base, because in both Staffa Group sample traverses T1 and T2, this is where the highest concentrations of K_2O occur".

Work carried out since this was reported has shown that this statement is incorrect. The remainder of this report presents new Ar/Ar data from traverses T1 and T2 and

12. Methodology

12.1. Field sampling

From Mull, basalt and sediment samples were collected from the Staffa and Plateau Group lavas. From the Faroe Islands basalt and sediment samples were collected from the Malinstindur and Enni Formations. The strategy for sampling was underpinned by the requirement to assess chemical and isotope variation throughout lavas and samples were taken at 0.5m or 1.0m intervals and converted to % height from lava base (each traverse from base to top of a lava is assigned a 'T' number). For GC-MS organic geochemistry measurements, sediment samples were taken from beneath each lava traverse, at the contact with the overlying lava. Samples for palynology were collected from appropriate sedimentary units beneath the lava traverse.

12.2. Sample screening

In the field the relative abundance and magnitude of any vesicles was noted for each sample within a traverse and the general characteristics of any infilling minerals. For a first-order screening in the laboratory, slabs were cut from every sample taking care to remove weathered outer surfaces. Thin sections were made and assessed for alteration and features that are likely to have a controlling effect on the Ar/Ar dating system. Using this approach two sections were chosen for detailed experimentation: Staffa Group lava in the vicinity of McCulloch's Tree (T1), and Staffa Group lava at Ardtun Head (T2). From the Malinstindur Formation two traverses have been selected, both from Svínair Quarry, Esturoy (T3, T4). From the Enni Formation one traverse has been selected, from Neshagi Peninsula, Esturoy (T5).

12.3. XRF preparation and analysis

T1-T5 samples were crushed by jaw-crusher and an aliquot milled to a fine powder. Glass disks and pressed powder pellets were made for XRF major and trace element analysis. Whole rock major and trace element concentrations were determined by XRF analysis undertaken on an ARL 8420+ dual goniometer wavelength dispersive XRF spectrometer. The spectrometer is equipped with a 3KW Rh anode end-window X-ray tube, and uses fully collimated flow proportional and scintillation counters. The machine is equipped with 5 diffraction crystals: multilayer AXO6, PET, Ge111, LiF200 and LiF220. Within each run, elemental intensities are corrected for background and peak overlap interferences. Medium-term instrumental drift is corrected for using a drift normalisation monitor built into the software. Matrix corrections for major elements use the Traill- Lachance procedure. Typical estimates of the precision of major element determination are ~ 0.18 – 0.73%. Monitor

samples used routinely at the OU were regularly included within the sample batches to ensure that there were no problems with either sample preparation or analysis.

12.4. Ar/Ar dating preparation and irradiation

T1 and T2 samples were crushed by jaw-crusher and an aliquot sieved to five size fractions that were repeatedly washed to remove dust. Aliquots of three size fractions were hand- picked using tweezers and a binocular microscope. Care was taken to select homogeneous basalt pieces that were representative of the size fraction, notably variation between size fractions were controlled by presence and abundance of organic-rich clay or zeolite vesicle fill.

The following statement occurs in section 12.4. of C46-41-01 interim report (1st June 2009):

"It is predicted that there will be a gradation in age – coarser size fractions that contain greater abundance of vesicle fill yielding older apparent Ar/Ar ages and more disturbed release spectra shapes than the finest size fraction".

We conclude from analysis of T1 and T2 Mull samples that this assumption is not supported by the data. Consequently the sample preparation for traverses T3-T5 has been streamlined by selecting the coarsest size fractions only. Once the samples were hand-picked (0.03 to 0.05g per sample) they were alternately washed in acetone and deionised water, and each sample packaged in Al foil for irradiation. Standard mineral GA1550 (age 98.79±0.96 Ma; Renne et al. 1998) was included either side of every 10 basalt samples to provide a monitor for neutron flux during the irradiation procedure. Samples were then sent to the McMaster reactor (Canada) for irradiation.

12.5. Palynology

Samples collected from the interbasaltic sedimentary successions were crushed and dissolved in hydrofluoric acid to remove silicates. After neutralisation, the residues were treated in dilute nitric acid to remove pyrite, the residue being mounted as strew mounts for analysis by transmitted light microscopy.

13. Mull Staffa Group Lava Results

13.1. Sample traverse: Mull T2 (Ardtun), A6 Staff Group lava

13.1.1 Individual Ar/Ar ages within T2

a

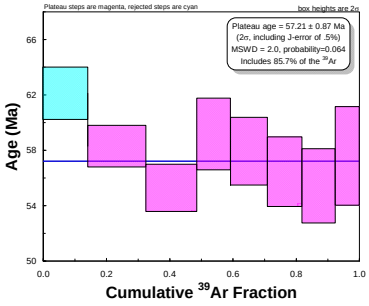

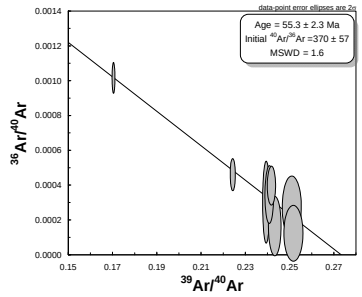

b

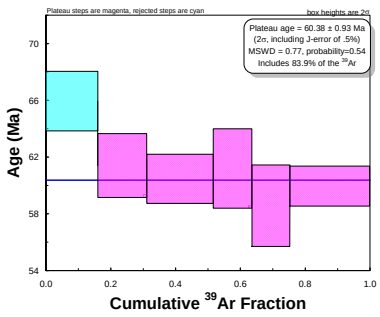

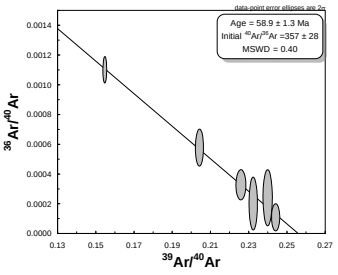

c

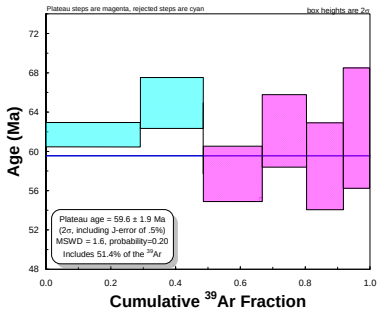

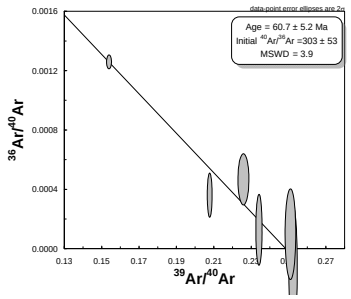

d

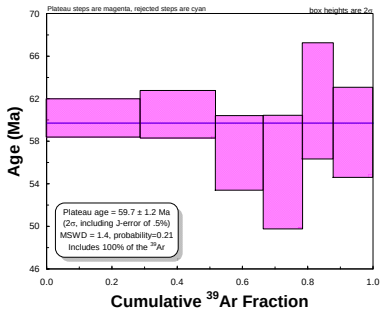

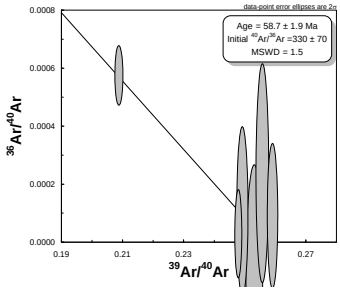

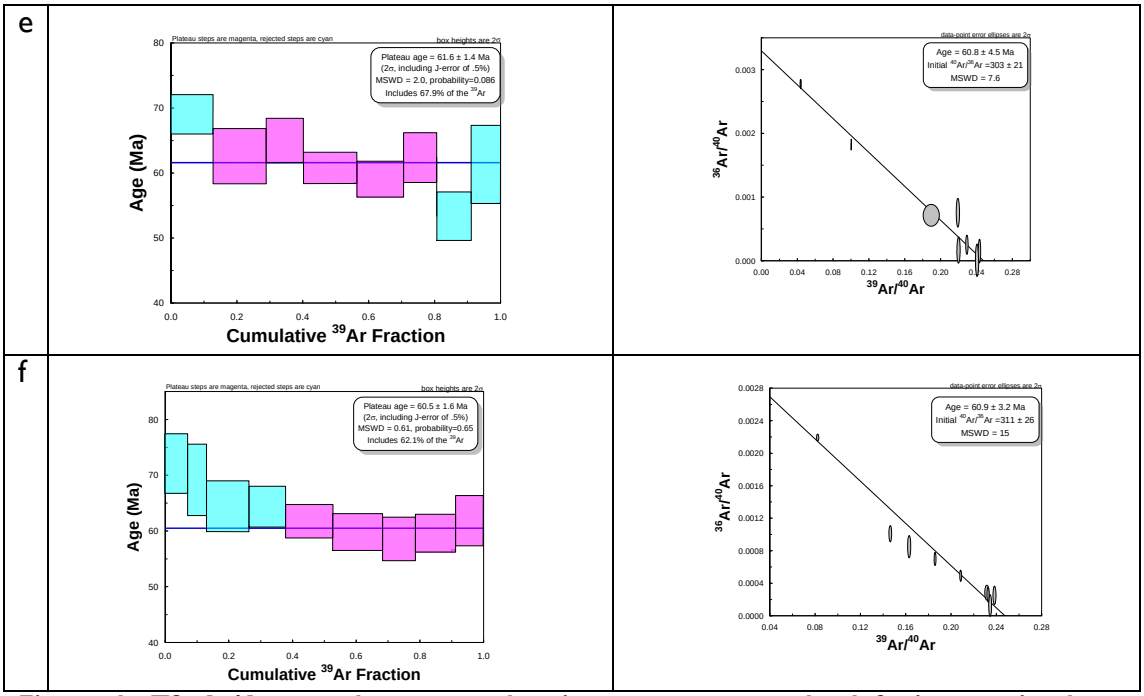

Figure 1. T2 Ar/Ar age data – step-heating spectrum on the left, inverse isochron correlation on the right, and ordered from lava base to lava top. a) A46 (base); b) A47; c) A48; d) A49; e) A50; f) A52 (top).

Figure 1a. A46 yields a plateau age of 57.2±0.9 Ma, and an isochron age of 55.3±2.3 Ma, both of which are within error of one another. The elevated age in the low-temperature release (first) step of the step-heating spectrum indicates the possible presence of excess argon in a low-retentive part of the whole rock, which could be alteration (sericite, clay minerals). The inverse isochron line gradient and intercept is controlled by the single datapoint that has low $^{39}Ar/^{40}Ar$ (and so low potassium) and high $^{36}Ar/^{40}Ar$ (high atmospheric argon). This datapoint is the ca. 62 Ma first heating step and so it is evident that there is a component of the whole rock that is low in potassium, high in atmospheric argon, and contains some excess argon, this is likely to be an alteration phase. Notably it is a superficial feature and does not pervade the sample (or it would be affecting the remaining heating steps).

Figure 1b. A47 yields a plateau age of 60.38±0.93 Ma, and the first age step is considerably older (ca. 66 Ma). The inverse isochron age (58.9±1.3 Ma) is within error and has a low MSWD, but the intercept falls below the $^{36}Ar/^{40}Ar$ value for air (0.0034) indicating a small amount of excess argon, most likely associated with alteration as indicated by the low potassium, high atmosphere age step, the low-temperature ca. 66 Ma age step.

Figure 1c. A48 yields a plateau age of 59.6±1.9 Ma, again there are elevated ages in the low-temperature parts of the spectrum, but affecting more than just the first step. The inverse isochron age is within error of the plateau age (60.7±5.2 Ma) but has a high MSWD indicating discordance within the sample. Notably many of the age steps have atmospheric argon measurements of within error of 0, and the line gradient and intercept is controlled by a single low potassium, high atmospheric step, which corresponds to the lowest-temperature release step and so is also likely to be due to alteration in the sample.

Figure 1d. The plateau age of 59.7±1.2 Ma encompasses 100% of the released ^{39}Ar, although there is clearly some minor discordance in the 50-80% gas release portions of the spectrum. The inverse isochron age (58.7±1.9 Ma) is within error of the plateau age, although many of the datapoints are within error of 0 for atsmospheric argon, and the gradient and intercept is controlled by the single low potassium, high atmospheric argon datapoint (the first step on the heating spectrum). Since the age spectrum contains 100% of the released argon, and the intercept on the Y axis on the isochron is significantly below the value for air, it is likely that this sample contains a minor component of homogeneously-distributed excess argon (which is distinct from the minor alteration-derived excess argon that just contaminates the first step of each spectrum).

Figure 1e. A50 has a plateau age of 61.6±1.4 Ma, and is more discordant than any of the previous samples – the first and final two steps are not included within the plateau age calculation. The isochron age (60.8±4.5 Ma) is within error of the plateau age. Notably this isochron is the only one whereby the intercept on the Y axis passes through the value for air, which would conventionally indicate that there is no excess argon in the sample. However, the lowest potassium, highest atmospheric argon step in this case, is the last step in the spectrum, not the first one, and taking this step out of the calculation yields an isochron age of 59.5±4.5 Ma, with an intercept of 0.0024 (within the realms of excess argon). To make sense of this, it is apparent that there is an additional component of argon in this sample that is associated with a highly retentive mineral within the whole rock, and is outgassing at high temperatures, but has an alteration-type signal (and is artificially skewing the isochron). At this stage it is not clear what this component is. The second high-atmosphere, low potassium point on the isochron is in fact that lowest-temperature release step which has a highly elevated age of ca. 70 Ma, indicative of excess argon associated with alteration.

Figure 1f. Sample A52 has a plateau age of 60.5±1.6 Ma and an inverse isochron age that is within error, at 60.9±3.2 Ma. There is evidence for greater discordancy in the low-temperature parts of the spectrum, the first 40% with elevated ages, as high as 75 Ma. The inverse isochron is also discordant and controlled by the single high atmospheric and low potassium datapoint, which equates to the lowest temperature release step that has the highest age. There is clear evidence for excess argon in the sample (based on the isochron intercept) that is homogeneously distributed within the whole rock.

13.1.1. Ar/Ar age variation within T2

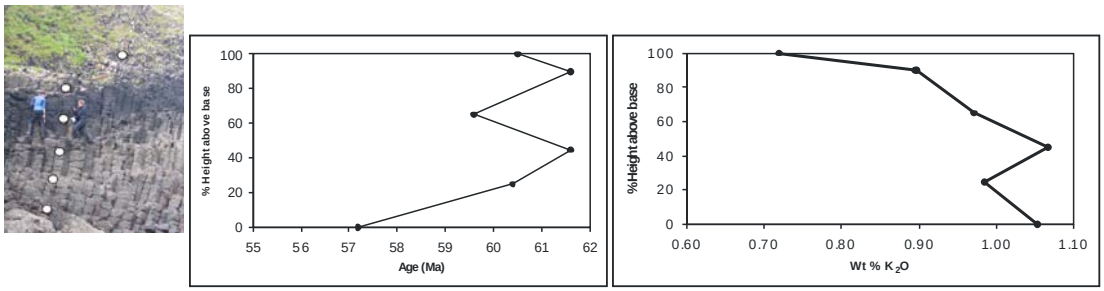

Figure 2. T2 field photograph, Ar/Ar ages and K_2O contents (error bars on the Ar/Ar ages are removed for clarity but fall within the < ± 1 Myr, 2σ).

The ages vary from base to (near to) the top of the lava (the actual lava top could not be sampled for safety reasons). There is a progression of age from base (57.2 Ma) to core (61.5 Ma; 50% height) and from here to 100 % height the ages vary from 59.4 Ma to 61.5 Ma. The bulk K2O pattern shows a marked decrease from top down to 50%, at which point there is a sharp decrease and then an increase at the base.

13.3. Sample traverse: Mull T1 (McCulloch's Tree) A6 Staffa Group lava

13.1.1. Individual Ar/Ar ages within T1

a	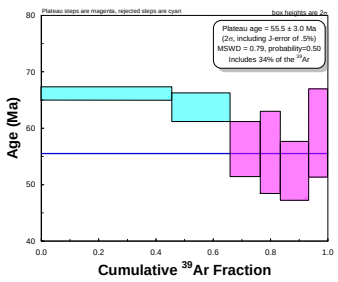	(could not construct isochron due to all steps having insufficient ^{36}Ar)
b	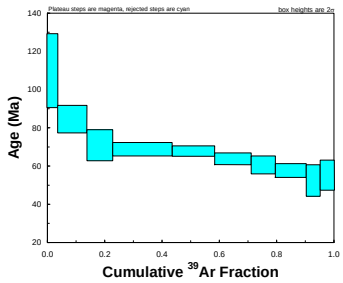	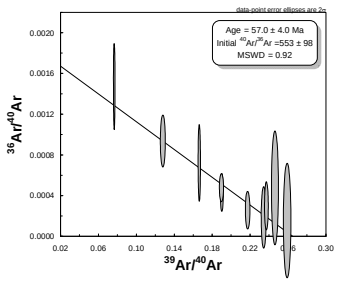
c	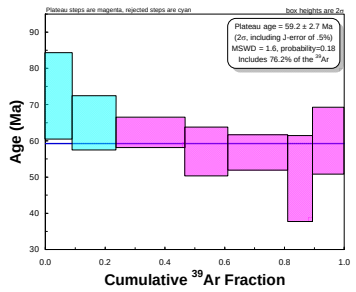	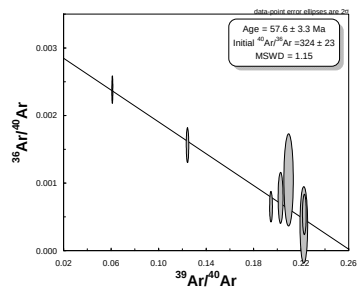
d	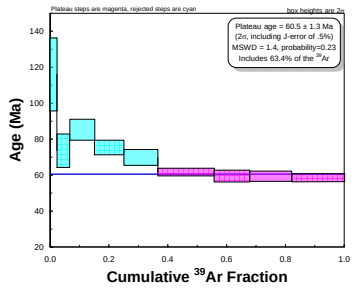	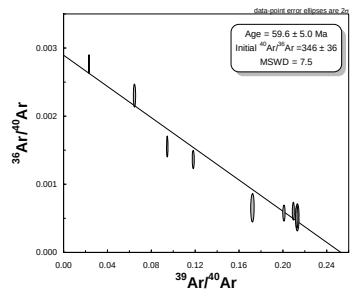

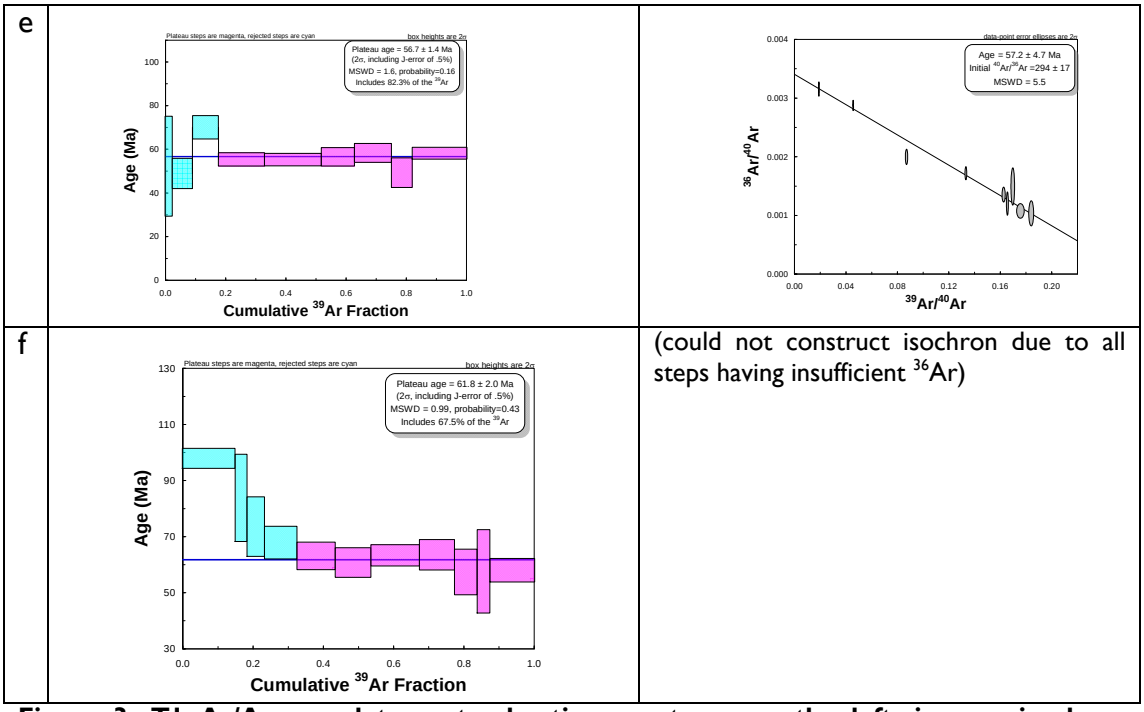

Figure 3. T1 Ar/Ar age data – step-heating spectrum on the left, inverse isochron correlation on the right, and ordered from lava base to lava top. a) B4 (base); b) AB5; c) B6; d) B7; e) B8; f) B9 (top).

Figure 3a. B4 has a plateau age of 55.5±3 Ma, and this is based on the final 34% of the gas released and so technically it does not conform to a statistically valid plateau age (50% of the gas released). However, it is indicative of a young age for the sample, but there is also evidence in the lower temperature release steps for excess argon in the form of elevated ages (ca. 65 Ma). The sample had insufficient atmospheric argon in it to enable the construction of the inverse isochron diagram.

Figure 3b. B5 did not yield a plateau age, or even a 'forced' plateau age that would be based on a slightly lesser percentage of gas yield than the accepted 50%. The ages vary from ca. 110 to 70 Ma in the first three release steps, and reduce to ca. 56 Ma in the final, high temperature steps. This is clearly a discordant sample with significant excess argon in the low- and mid-temperature release steps. The inverse isochron age of 57.0±4.0 Ma suffers from the problem of the intercept on the Y axis being significantly lower than the value for air (0.0034) which strongly indicates the presence of a small amount of excess argon in the sample.

Figure 3c. B6 yields a plateau age of 59.2±2.7 Ma and has two slightly elevated ages in the first two steps (ca. 65 Ma and ca. 75 Ma), corresponding to the two low potassium, high atmospheric argon steps in the isochron diagram. The isochron age (57.6±3.3 Ma) is within error of the plateau age, however, there is evidence for the presence of a minor component of excess argon related to alteration in the low temperature steps.

Figure 3d. B7 yields a plateau age of 60.5±1.3 Ma. The spectrum is discordant with very elevated ages within the first 40% of the gas released. The inverse isochron correlation diagram demonstrates a sample that is well mixed between radiogenic and atmospheric argon (spread along a line) although some minor discordancy. The

isochron age of 59.6±5.0 Ma is within error of the plateau age, and the intercept on the Y axis is controlled by the low temperature (highest age) steps and so there is evidence for minor excess argon contamination.

Figure 3e. B8 yields a plateau age of 56.7±1.4 Ma and the 83% of the release spectrum on which this age is based is remarkably concordant, with only minor disturbance in the first three release steps, where ages vary between ca. 70 Ma and ca. 50 Ma. The inverse isochron age (57.2±4.7 Ma) is within error of the plateau age and intercepts the Y axis at the value for air, with an appropriate degree of spread (mixing) along the line. There is evidence for minor excess argon, most likely related to alteration, and being released at low temperatures.

Figure 3f. B9 yields a plateau age of 61.8±2.0 Ma, and there is strong discordance in the first 30% of the release pattern with ages as high as ca. 100 Ma. There was insufficient atmospheric argon within this sample to construct the inverse isochron correlation diagram, but based on experience of the other samples it is likely that the first four steps would correspond to low potassium values.

13.2.2 Ar/Ar age variation within the lava

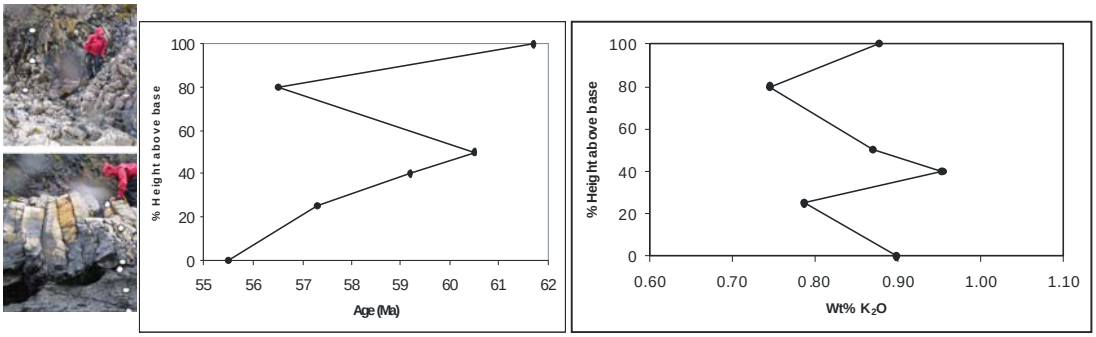

Figure 4. T1 field photograph, Ar/Ar ages and K_2O contents (error bars on the Ar/Ar ages are removed for clarity but fall within the < ± 1 Myr, 2σ).

The ages vary from base to (near to) the top of the lava (the actual lava top could not be sampled for safety reasons). There is a progression of age from base (55.5 Ma) to core (60.5 Ma; 50% height) and to 100 % (61.5 Ma) with a 'dip' in age at 80% (56 Ma). This pattern is also observed in the bulk K_2O values, the only divergence being at the base.

13.3. Comparison of T1 and T2

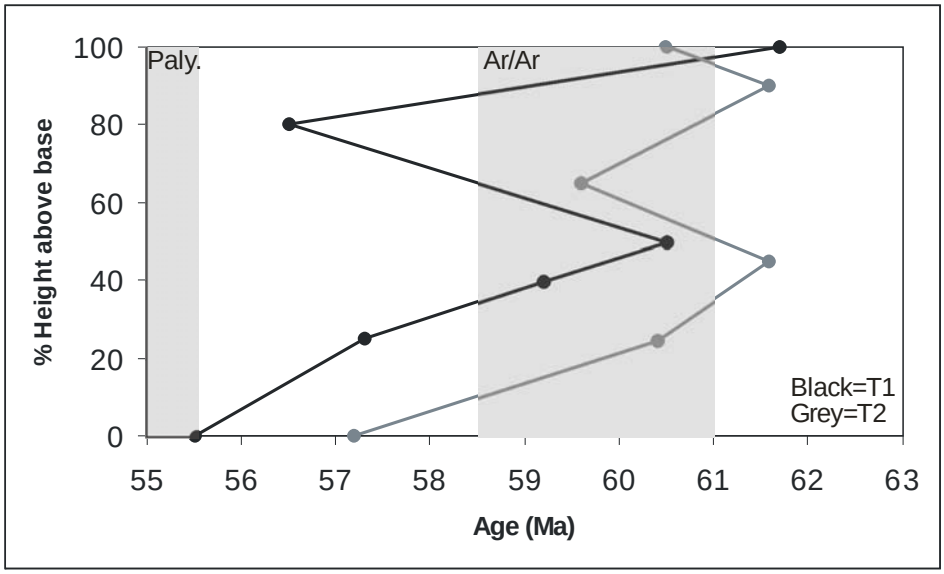

Figure 5. Comparison of T1 and T2 Ar/Ar ages, with grey boxes representing the age range derived from palynology, and the published Ar/Ar age range that is generally accepted as being representative of the time of eruption.

Notably the two traverses yield the same Ar/Ar age variation. Whilst this *might* be expected for two different parts of the same lava, these two sections are different thicknesses (T1=ca. 3m, T2=ca. 5m thick). The key point is that regardless of thickness the lava should yield the same Ar/Ar age from top to bottom since it was emplaced and cooled within a few thousand years, and this is not the case, there is a strong variation in Ar/Ar age from bottom to top of the lava.

The published Ar/Ar ages for these lavas are:

- 60.6 ± 0.3 Ma 'near base' of MPLF (Chambers & Pringle, 2001)
- 58.4 ± 0.2 Ma (wtd mean of 2 ages) '700m above base' MPLF (Chambers & Pringle, 2001)
- 58.7 ± 1.1 Ma 'within same lavas as Chambers & Pringle (2001)' (Ganerød et al., 2008)

Of concern is the use, in the literature, of the two ages published in Chambers & Pringle (2001) for calculating the eruption rate of the 700m of lava pile that intervene the two samples. Any use of published Ar/Ar data from the NAIP must be used with extreme caution, given that within individual lavas we have identified an age range spanning 6 Myr – encompassing the entire gamut of ages for phases 1 and 2 of NAIP volcanism.

In terms of understanding how inaccurate the Ar/Ar ages can be, the published palynological age for these Mull lavas is: 54.0 to 55.5 Ma (Jolley, 1997). The data from T1 and T1 are within error of this value at the base of the lava. We believe that this can be interpreted in the context of lava cooling, since both sections of lava were erupted into water and so the lava bases would have the highest cooling rate. Of note is the fact that the highest ages are within the cores of the lavas, which is where, conventionally, samples are collected for Ar/Ar dating.

13.4. Sample traverse: Mull T3 (Green Point) base Plateau Group lava

13.4.1. Individual Ar/Ar ages within T3

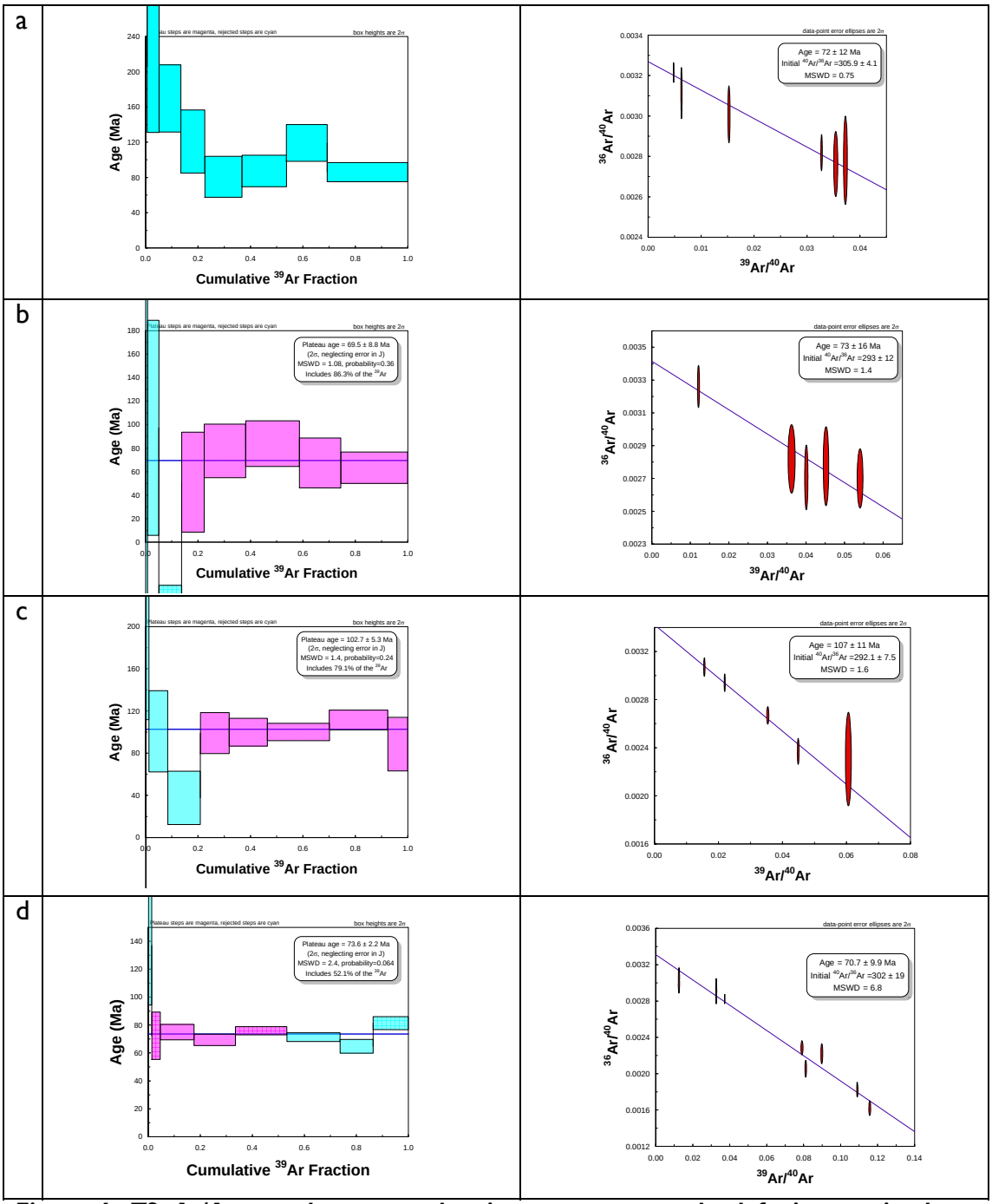

Figure 6. T3 Ar/Ar age data – step-heating spectrum on the left, inverse isochron correlation on the right, and ordered from lava base to lava top. a) M41 (base); b) M42; c) M43; d) M44 (top).

Figure 6a. Sample M41 does not yield a plateau age but has an inverse isochron correlation age of 72±12 Ma with an intercept within error of the value for air.

Figure 6b. Sample M42 yields a plateau age of 61±8 Ma and an inverse isochron age of 73±15 Ma. These values are within error of one another, notably the isochron age is strongly influenced by a single datapoint that has very low ^{39}Ar/^{40}Ar and high

$^{36}A/r^{40}Ar$ ratios indicating that it is low in potassium and high in atmospheric argon and so is likely to represent some alteration of the sample. This corresponds with the first heating step (the lowest temperature).

Figure 6c. Sample M43 yielded a plateau age of 103±7 Ma and an inverse isochron age of 107±11 Ma. Again these are within error of one another but significantly older than the other three samples. There is nothing notable within the data to indicate any disturbance to the argon system in this sample, although it is clearly much older than is geologically feasible.

Figure 6d. Sample M44 yields a plateau age of 74±2 Ma and an inverse isochron age of 71±10 Ma, again these are within error of one another. This sample appears to be slightly more disturbed than previous samples, identified by the two to three datapoint 'groupings' in the isochron diagram.

13.4.2 Age variation within T3

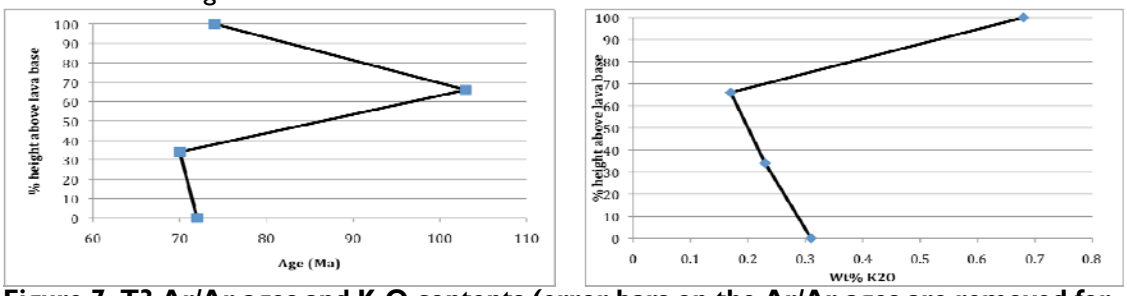

Figure 7. T3 Ar/Ar ages and K_2O contents (error bars on the Ar/Ar ages are removed for clarity but fall within the < ± 8 Myr, 2σ).

The T3 base Plateau Group lava in Figure 7 varies little in age about ca. 70 Ma with the exception of the core of the lava which has a highly elevated age of ca. 107 Ma, this datapoint corresponding to the lowest $\%K_2O$ value. As with the Staffa Group lavas from higher up in the volcanic sequence (T1 and T2) the ages are older than the ca. 55 Ma for the Group, notably T3 is consistently older than T1 and T2, but the similarity between all three traverses lies in the oldest ages appearing in the core of the lava.

13.5 Preliminary model for T1 and T2

To try to understand the Ar/Ar age variation we draw on the model of Lyle (2000) for the cooling of multi-tiered lavas erupted into upland wet environments (as is comparable for the Mull and FIBG lavas).

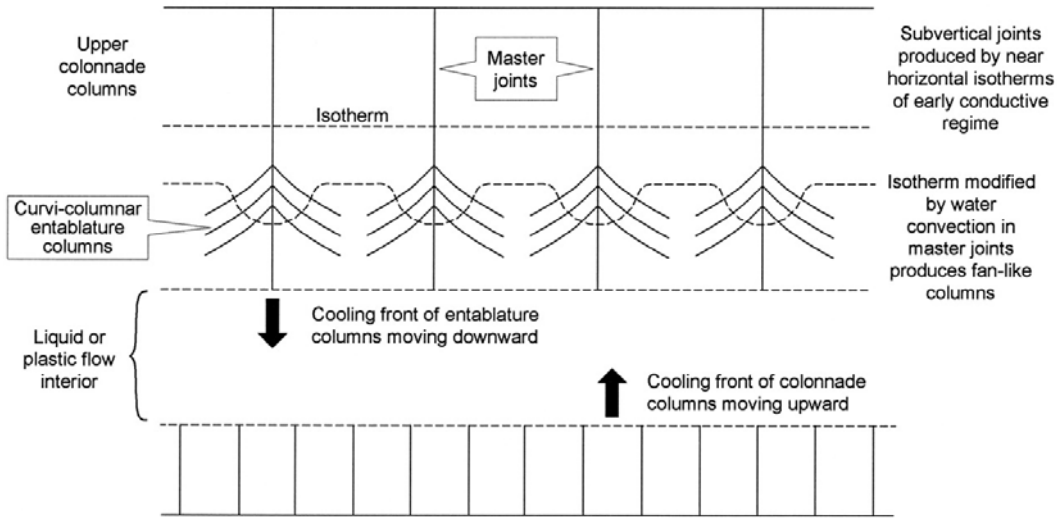

Figure 8. Model for cooling in multi-tiered lavas erupted into water-rich upland environments (from Lyle 2000).

Here, there are two cooling fronts moving towards the core of the lava. Top down the cooling front is enhanced by the influx of surface waters down through cooling joints. From the base up cooling is aided by rapid chilling at the base, as the lava comes into contact with surface waters. The area in the core of the lava where the cooling fronts converge is the part with the lowest cooling rate, and will remain liquid/plastic for longest. Given that the behaviour of argon is strongly controlled by temperature, this is of importance.

Figure 9 is the superimposition of the Ar/Ar data for T1 and T2 onto the cooling model of Lyle (2000).

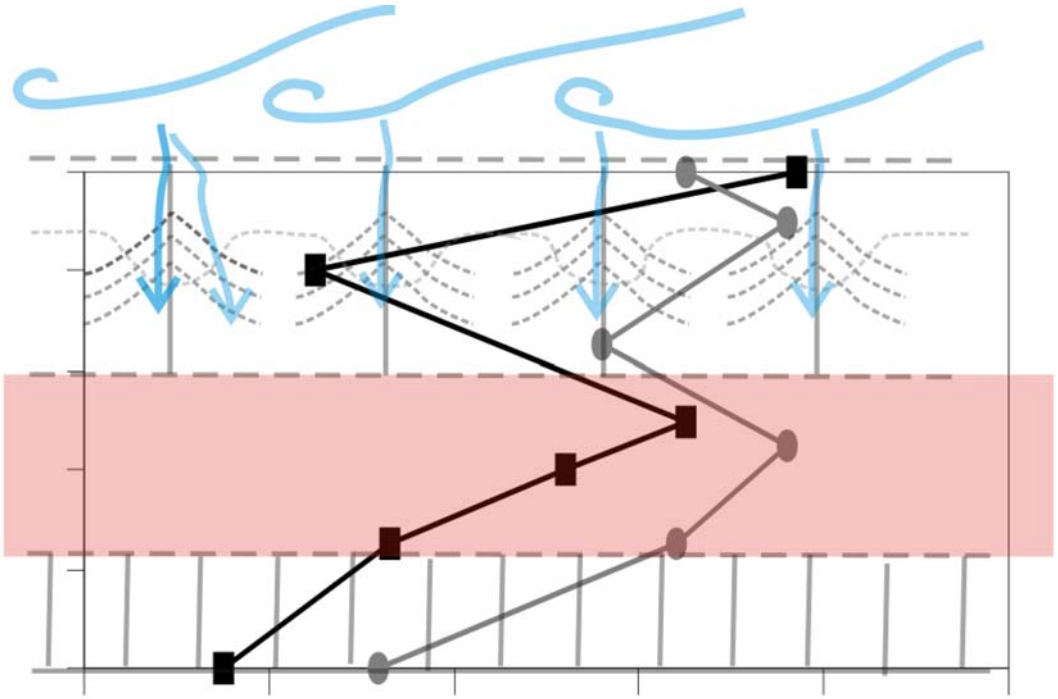

Figure 9. Superimposition of T1 and T1 Ar/Ar ages on to an appropriately scaled (relative to the Mull lavas sampled) version of the model of Lyle (2000).

The lava base corresponds to the lava quenched in contact with surface water, this quenching appears to have 'sealed' the Ar/Ar system, enabling the preservation of accurate Ar/Ar ages. The top of the lava is variously disrupted by weathering processes, the differences between T1 and T2 are controlled by the environment – T1 has a high biomass, low saturation environment and so weathering is more dominated by physical weathering and acid leaching, whilst in T2 the environment is more low biomass, high saturation, and so 'weathering' is dominated by leaching by surface waters. The core of the lava is where the ages are the most elevated, there is the highest concentration of excess argon, and the lowest cooling rate. This is important for the distribution of excess argon that is not brought in externally, at a late stage, by alteration of the basalt. It is likely to relate to the magma chamber. There are two possibilities: i) the lava was relatively poorly degassed with respect to argon, or, ii) the argon that is derived from the decay of potassium in nature, and would 'escape' the lava whilst at temperatures over ca. 250°C, was not able to escape because the base was sealed, and the top was sealed by rapid cooling in air, aided influxing surface waters. The highest bulk K_2O values correlating with the core of the lava and the highest ages indicates 'closed system' excess argon, derived from radiogenic argon that couldn't escape the lava (this is based on the theory that I have developed for other types of rock – metamorphic and igneous: e.g. Sherlock & Kelley, 2002). However, our work on Icelandic lavas indicates that whilst it is possible to outgas volatile species such as H_2O and CO_2 from a magma during eruption, the outgassing of magma chamber derived argon is far less efficient and it remains within the lava. We interpret the Ar/Ar variation in T1 and T2 as remnants of magma chamber argon that did not degas, and was migrating towards the warmest parts of the lava as it cooled, concentrating in the core.

13.5.1. Consideration of T3 in light of the model for T1 and T2

T3 is from what is considered to be the base of the Plateau Group Lavas and is considerably and consistently older than the T1 and T2 lavas from Staffa Group lavas later in the eruption sequence. The age variation in T3 is comparable to T1 and T2 and so the same model is applicable, but the much older ages relate to a higher concentration of excess argon in this lava. From the field observations the lava is neither vesicular nor does it contain zeolites implying that it is less degassed than T1 and T2, or undegassed. The higher concentration of excess argon in this sequence relates to the degassing history of the lava.

13.6. Implications of T1, T2 and T3 data for regional correlation

Figure 10 below is an extract from Chambers et al (2005) the accepted standard for wider NAIP correlation. The Mull lavas, based on the Ar/Ar ages of Chambers & Pringle (2001), are correlative with lavas in Skye, the Small Isles and Antrim, attributable to Phase 1 volcanism. The palynological data from Mull indicate that the lavas are correlative with the Sele Formation (Jolley, 1997), some 4-5 Myr earlier and more aligned with Phase 2 volcanism. It is likely that the variance in Ar/Ar data in Mull lavas is not restricted to Mull, and that Ar/Ar data from Phase 1 volcanic centres might also be severely problematic, including the Lopra Formation. The data from T3 base of the Plateau Group is not considered to be representative of the timing of volcanism, but due to excess argon in the magma chamber residing in an undegassed lava.

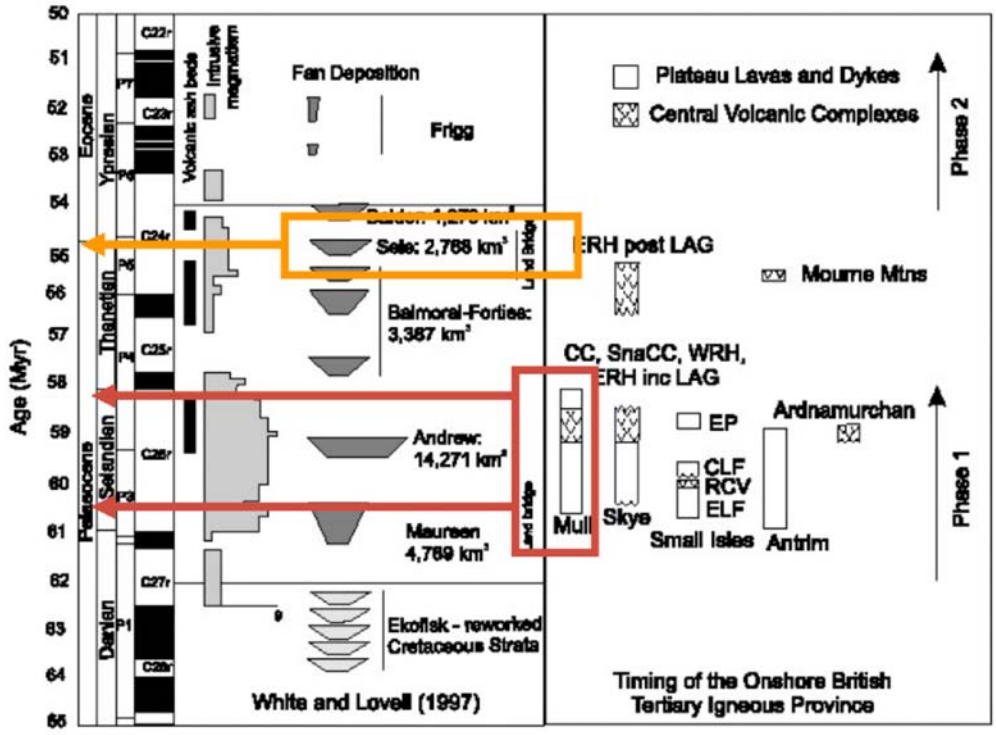

Figure 10. (From Chambers et al., 2005) A schematic representation of the onshore magmatic activity of the BTIP, taken from this study (Chambers et al., 2005), Chambers and Pringle (2001), Chambers (2000), and Gamble et al. (1999) compared to the correlation of sand pulses in the North Sea and intrusive magmatism redrawn from White and Lovell (1997). The time scale of Berggren et al. (1995) is used and the arrows mark the two phases of magmatism (Saunders et al., 1997). CC—Cuillin Centre; SnaCC—Strath na Creitheach Centre; WRH—Western Red Hills; ERH—Eastern Red Hills; LAG—Loch Ainort Granite; EP—Sgurr of Eigg pitchstone; CLF—Canna Lava Formation; RCV—Rum central volcano; and ELF—Eigg Lava Formation. The dominant style of magmatism changes during the development of the province, and it approximately correlates to some of the sand bodies in the North Sea. For example, the onset of magmatism in the BTIP corresponds to the first sand pulse in the North Sea (Maureen), but magmatism continues when there is no sediment in to the North Sea. Nevertheless, the largest sand pulse (Andrew) is contemporaneous with the development of central volcanoes of Mull and some of Skye. Red box: Ar/Ar age range for Mull lavas; Orange box: palynological age and correlation with the Sele Formation (Jolley, 1997).

14. Faroe Island Basalt Group Results

14.1 T4 and T5 Svinair Quarry, Malinstindur Formation

Figure 11. Svinair Quarry located on the west side of Esturoy 3km north of the Streymoy road bridge. The left hand panel is the northwestern end of the exposure (T4), the right hand panel is the southeastern end (T5).

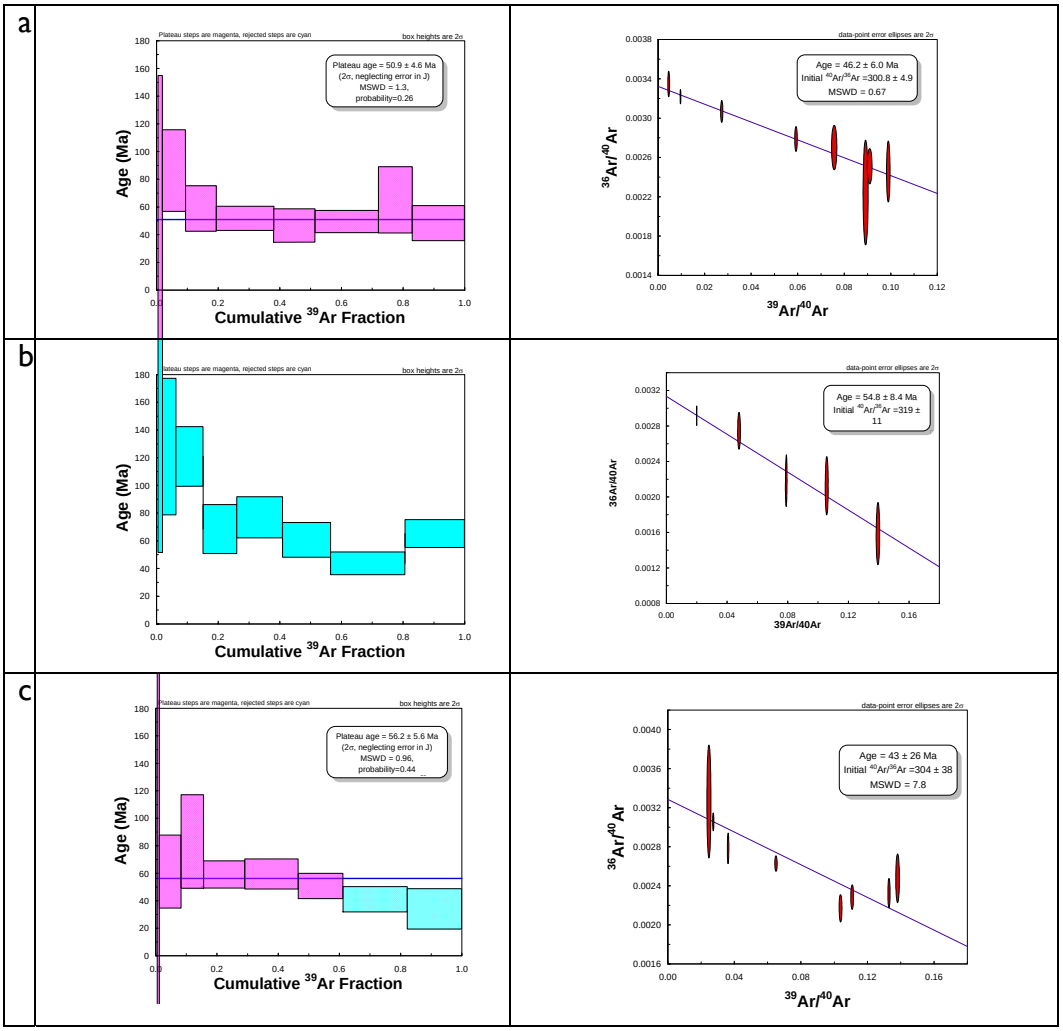

d	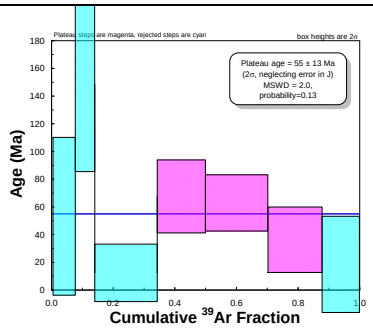	Data do not define isochron.
e	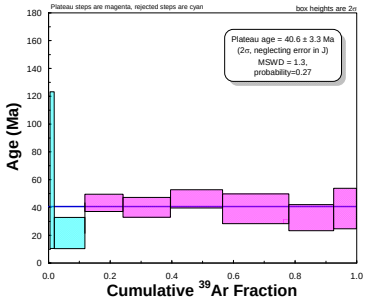 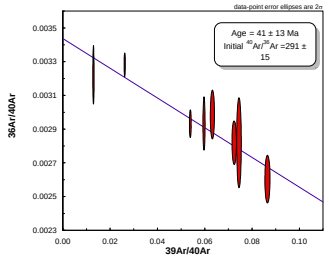	
f	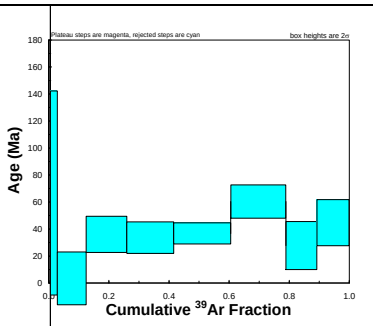	Data do not define isochron.
g	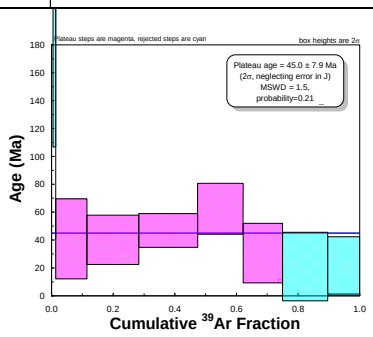	Data do not define isochron.
h	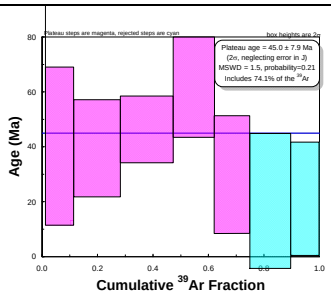	Data do not define isochron

Figure 12. Ar/Ar data from T4, Svinair Quarry, Malinstindur Formation

Figure 12a. Sample F71 has a plateau age of 51±5 Ma comprising 100% of the released gases. The inverse isochron has an age of 46±6 Ma, within error of the plateau age.

Figure 12b. Sample F72 does not define a plateau, the low-temperature release steps are very high and indicate that the sample contains some excess argon in low-retention minerals (alteration products). The inverse isochron has an age of 55±8 Ma, the intercept is slightly lower than the value for air (0.00344) although is within error of air, indicating a possible minor component of excess argon.

Figure 12c. Sample F73 has a plateau age of 56±6 Ma, comprising 61% of the released gas. The inverse isochron indicates internal discordancy in the sample – the low ^{39}Ar and high ^{36}Ar steps indicative of alteration. In spite of the discordancy the high error renders the isochron as being within error of the plateau age.

Figure 12d. Sample F74 yields a plateau age of 55±13 Ma comprising 54% of the released gas. The sample is strongly discordant and there is evidence for excess argon in the lower temperature steps. The data did not define an isochron.

Figure 12e. Sample F75 has a plateau age of 41±3 Ma, and an isochron of 41±13 Ma, within error of the plateau age. The isochron demonstrates discordancy with a dominant group of data with higher ^{39}Ar values and two datapoints with low ^{39}Ar and high ^{36}Ar, corresponding to the two low-temperature steps in the step-heating spectrum.

Figure 12f. Sample F76 is a strongly discordant sample that yields neither a plateau age nor isochron. The ages are in the 40-60 Ma age range.

Figure 12g. Sample F77 yields a plateau age of 45±8 Ma, comprising 74% of the released gas. This samples is also discordant the data do not define an isochron.

a	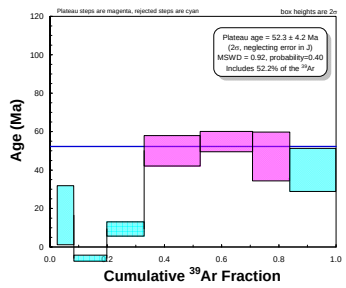	Data do not define isochron
b	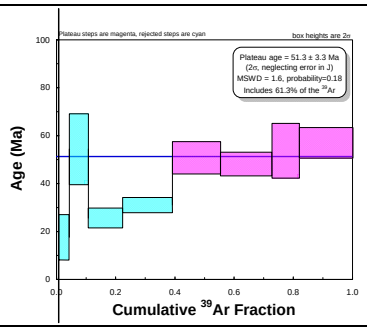	Data do not define isochron

c	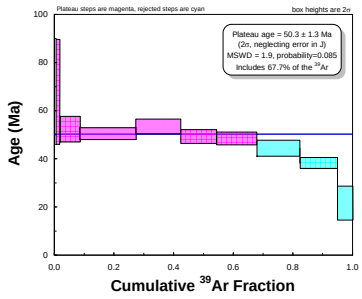	Data do not define isochron
d	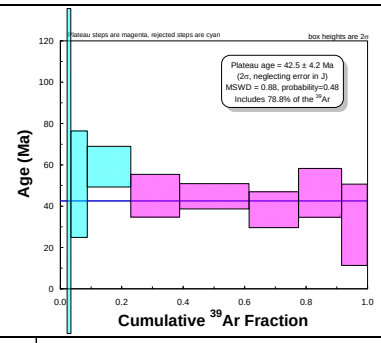	Data do not define isochron
e	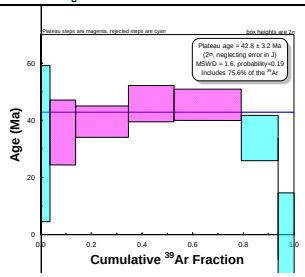 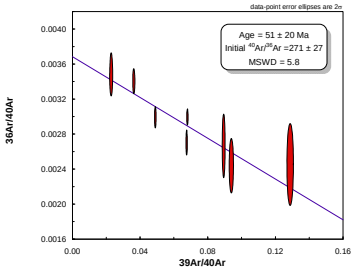	
f	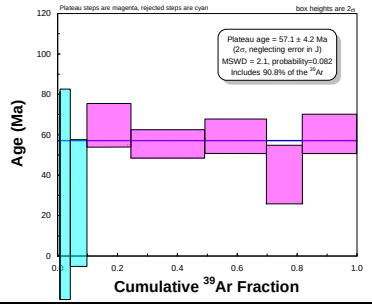	Data do not define isochron
g	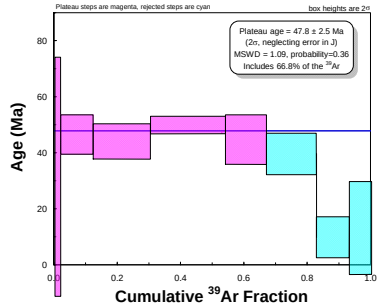	Data do not define isochron

h	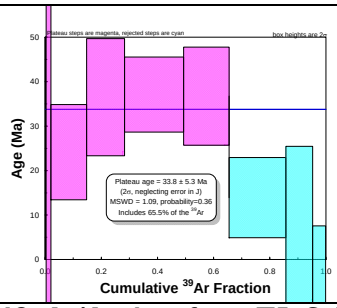	Data do not define isochron

Figure 13. Ar/Ar data from T5, Svinair Quarry, Malinstindur Formation

Figure 13a. Sample F79 has a plateau age of 52±4 Ma and comprises 52% of the released gases. The spectrum indicates that the sample is strongly discordant with significant argon loss in the low-temperature steps. The isochron echoes this and is dominated by a small number of datapoints with high errors and one with very high ^{36}Ar, giving an age of 44±27 Ma (within error of the plateau age).

Figure 13b. Sample F80 has a plateau age of 52.3±4.2 Ma comprising 52% of the released gases. Argon loss is observed in the low temperature steps in this sample. The data did not define an isochron.

Figure 13c. Sample F82 has a plateau age of 50.3±1.3 Ma comprising 68% of the released gases and with argon loss observed in the high temperature steps. The data did not define an isochron.

Figure 13d. Sample F83 has a plateau age of 42.5±4.2 Ma comprising 80% of the released gases and with argon loss observed in the low temperature steps. The data did not define an isochron.

Figure 13e. Sample F84 has a plateau age of 42.8±3.2 Ma comprising 76% of the released gases and with argon loss observed in the high temperature steps. The data defined an isochron age of 51±20 Ma but the high MSWD indicates strong discordancy within the sample.

Figure 13f. Sample F85 has a plateau age of 57.1±4.2 Ma comprising 91% of the released gases and with minor argon loss observed in the low temperature steps. The data did not define an isochron.

Figure 13g. Sample F86 has a plateau age of 47.8±2.5 Ma comprising 67% of the released gases and with argon loss observed in the high temperature steps. The data did not define an isochron.

Figure 13h. Sample F87 has a plateau age of 33.5±5.3 Ma comprising 66% of the released gases, there is very significant argon loss in the high temperature steps. The data did not define an isochron.

14.2 Neshagi Peninsula T6 (C+2 below Argir Beds, Enni Formation).

Good example of lava emplaced into wet sediment. 3m-thick aphyric lava overlies > 50 cm-thick fluvial sediment. The contact is irregular and sediment 'flames' into base of lava, and lava base ha a 10cm-thick zone of micro autobrecciation.

Figure 14. T6 at Neshagi Peninsula, southern tip of Esturoy.

a	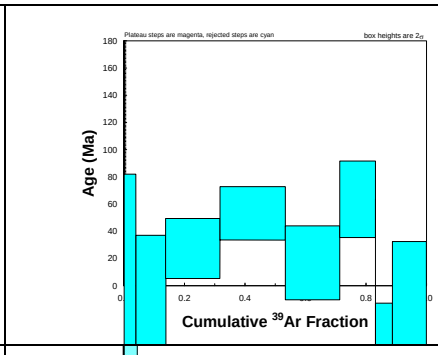	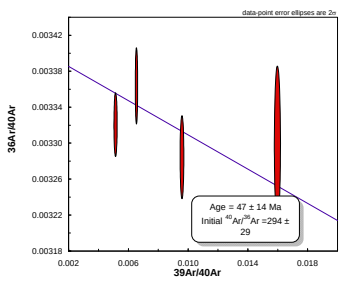
b	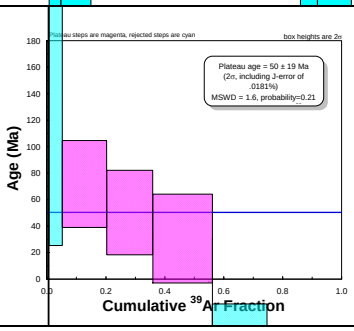	Data do not define an isochron.

c	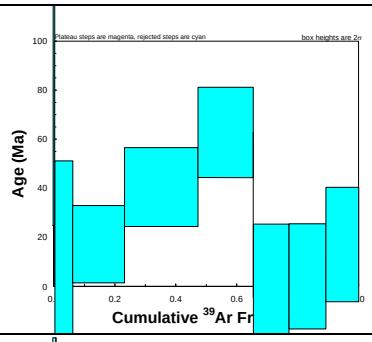	Data do not define an isochron.
d	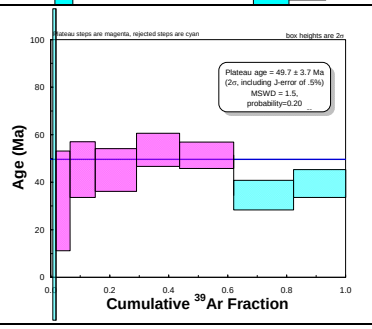	Data do not define an isochron.
e	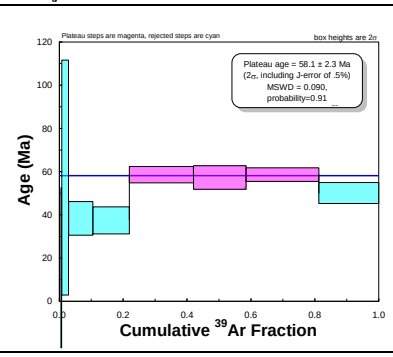 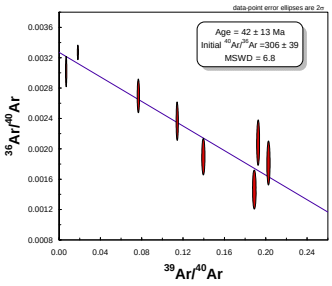
f	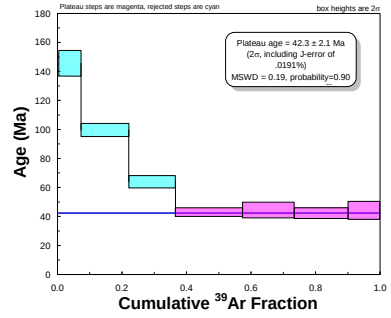 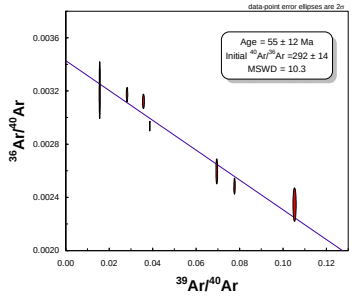
g	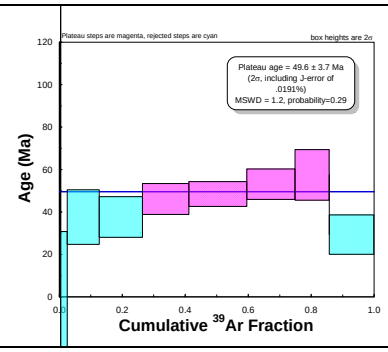 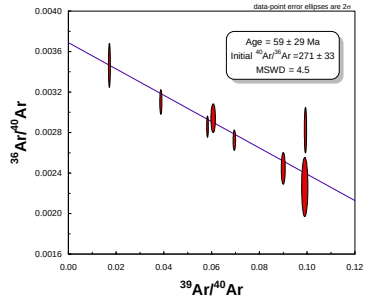

h	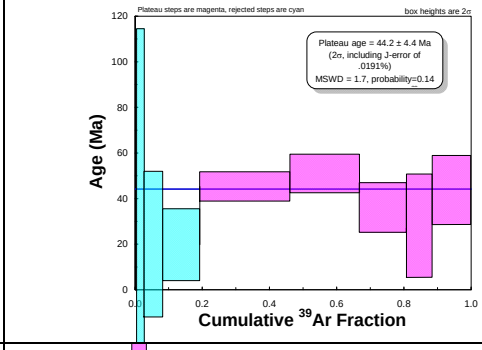	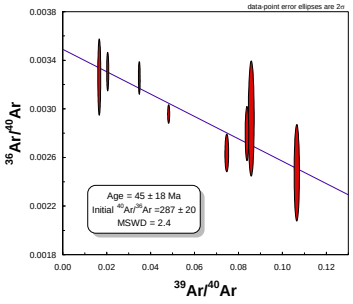
i	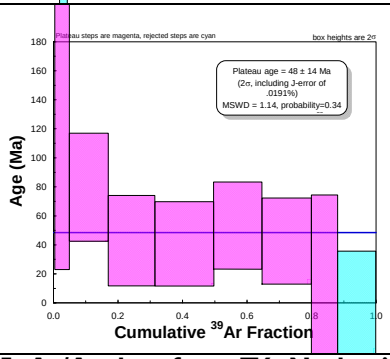	The data do not define an isochron.

Figure 15. Ar/Ar data from T6, Neshagi peninsula, Enni Formation

Figure 15a. Sample F59 does not define a plateau age, the sample is strongly discordant with individual steps varying from neagative to ~ 60 Ma in age. The isochron age is also strongly discordant and those steps that are not negative in age are used, the isochron age is 47±14 Ma.

Figure 15b. Sample F60 has a plateau age of 50±19 Ma, this is not a statistically viable plateau age since it comprises less than 50% of the released gases, though it is indicative of the age of the sample. It is strongly discordant with significant argon loss in the high temperature steps. The data do not define an isochron.

Figure 15c. Sample F61 does not define a plateau age, the sample is strongly discordant with individual steps varying from neagative to ~ 60 Ma in age. The data do not define an isochron.

Figure 15d. Sample F62 has a plateau age of 49.7±3.7 Ma comprising 60% of the released gases and with minor argon loss in the high temperature steps. The data do not define an isochron.

Figure 15e. Sample F63 has a plateau age of 58.1±2.3 Ma comprising 50% of the released gases and with minor argon loss in the low temperature steps. The isochron age is 42±13 Ma and indicates that the sample is strongly discordant, dominated by two very high atmospheric points that are low in potassium, corresponding to those points that display argon loss.

Figure 15f. Sample F64 has a plateau age of 42.3±2.1 Ma comprising 65% of the released gases and with excess argon in the low temperature steps. The isochron age is 55±12 Ma and indicates that the sample is strongly discordant.

Figure 15g. Sample F65 has a plateau age of 49.6±3.7 Ma comprising 65% of the released gases and with argon loss in the low and high temperature steps. The isochron age is 59±29 Ma and indicates that the sample is discordant.

Figure 15h. Sample F67 has a plateau age of 44.2±4.4 Ma comprising 80% of the released gases and with argon loss in the low temperature steps. The isochron age is 45±18 Ma and indicates that the sample is moderately discordant.

Figure 151. Sample F68 has a plateau age of 48±14 Ma comprising 90% of the released gases and with argon loss in the high temperature steps. The data do not define an isochron.

14.3 Esturoy Tunnel T7, Malinstindur Formation

Figure 16. Sample site from Esturoy Tunnel, Malinstindur Formation. Two samples were taken at intervals down from the top of the lower lava, and up from the base of the overlying lava, there being a narrow (20cm) fluvial volcanoclastic sandstone between the two lavas.

a

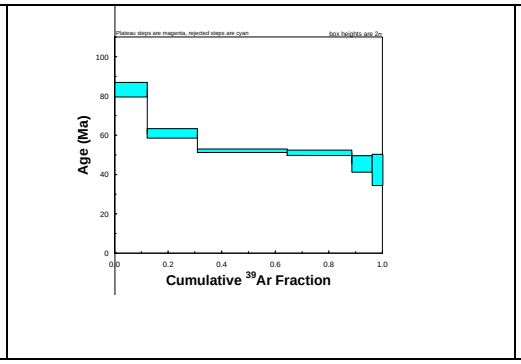

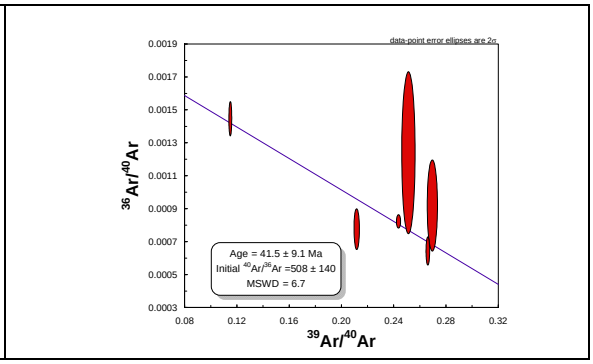

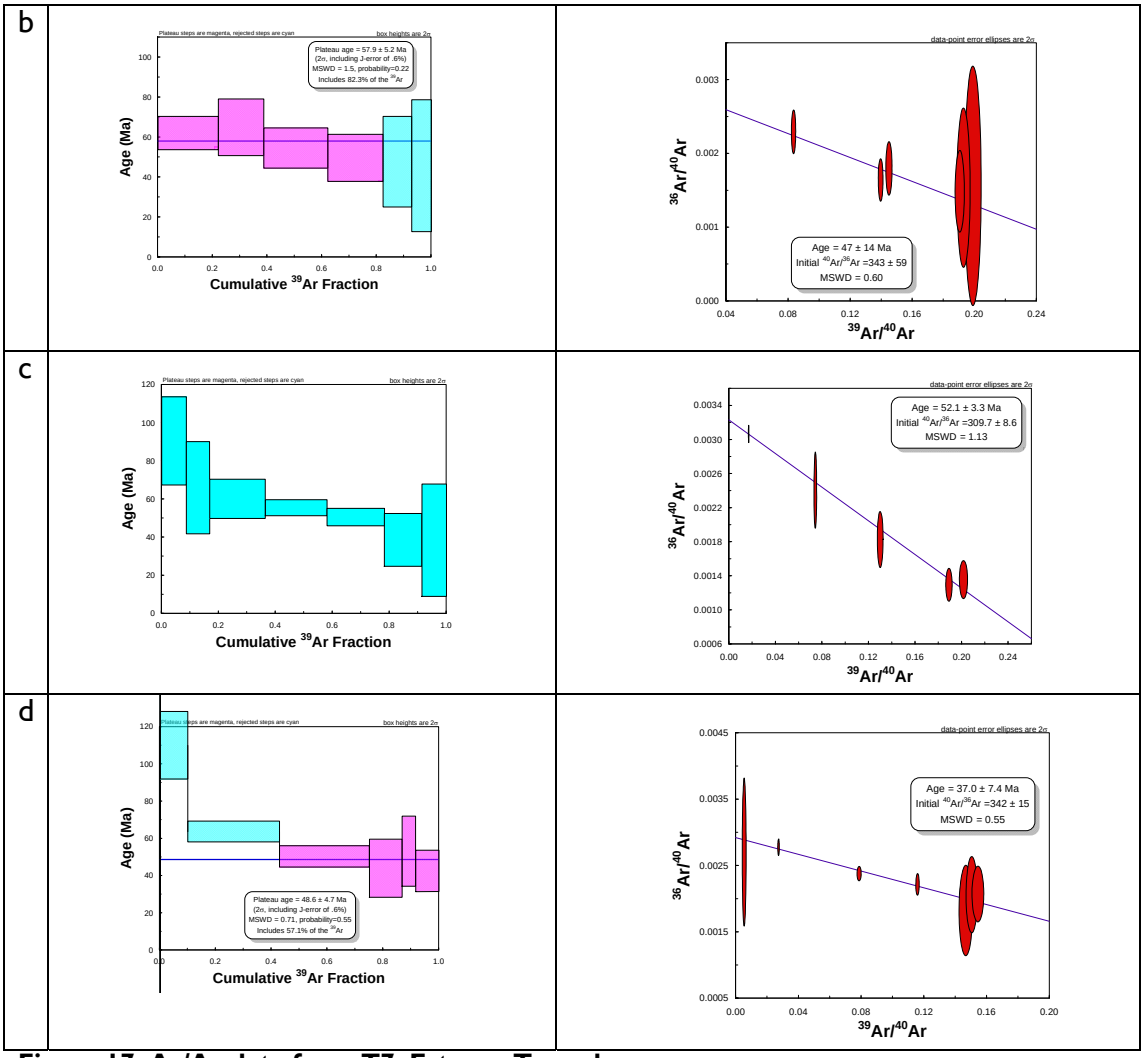

Figure 17. Ar/Ar data from T7, Esturoy Tunnel.

Figure 17a. Sample F59 does not define an plateau age and the individual steps range in age from ca. 45 to 82 Ma. The isochron age is 41.5±9.1 Ma and the sample is discordant.

Figure 17b. Sample F60 has plateau age of 57.9±5.2 Ma comprising 82% of the released gases, and within an isochron age of 47±14 Ma.

Figure 17c. Sample F62 does not define an plateau age and the individual steps range in age from ca. 40 to 100 Ma. The isochron age is 52.1±3.3 Ma and the sample is discordant.

Figure 17d. Sample F63 has plateau age of 48.6±4.7 Ma comprising 57% of the released gases, and within an isochron age of 37±7.4 Ma.

15. Palynology

15.1 *Mull T1 (McCulloch's Tree)*

MacCulloch's tree (a fossilised tree) exists as a cast surrounded by columnar basalt of the A6 flow, Palaeogene Staffa Formation (Jolley et al. 2008). Half a kilometre south along the coast from the tree are a series of distinctive jointing patterns within the same lava flow. These patterns appear as thin joint-columns spreading out from a spherical centre. The distinct shape of the jointing patterns have led to them being referred to as 'wagon-wheel structures' in the remainder of this report. Considering their proximity to the fossil tree, as well as the similarities seen in the jointing patterns of the wagon wheels and the lava jointing adjacent to the fossil tree, it may be possible that the two represent related palaeo-features (i.e. trees). The varying diameters of the jointing influence of the objects could possibly relate to the size of the objects (trees) that the lava was flowing around. However, it is most likely a result of the destruction of outcrop by shore-related processes.

The nature of the jointing, with cracks initially forming at right angles to the centres, and eventually curving upwards, is similar to that seen around the fossilized tree. An approximately 30cm thick humic coal bed is present around the west coast of Mull where the above mentioned fossilised tree are also located. This coal seam, along with an underlying tuff layer, is adjacent to the hyaloclastites that encased the trees and formed the wagon-wheel structures. The coal and tuff layers most likely represent the material that the forest was growing in, and hence spore and pollen analysis of these layers should provide one with the necessary information required for predicting the nature of the forest. Results from this analysis indicated the following six dominant pollen and spore types (Table 1):

Table 1 pollen types from McCulloch's Tree locality

	Spore / Pollen type	No. of Grains
1	*Inaperturopollenites hiatus*	141
2	*Nyssapollenites kruschii*	13
3	*Laevigatosporites / Deltoidospora*	13
4	*Pityosporites*	4
5	*Alnipollenites verus*	5
6	*Caryapollenites*	3

This area will mainly have included the 20-25m tall *Nyssa* trees (tupelos). Sporadically spread among them would have been hickory- (*Caryapollenites*) and small pine- (*Pityosporites*) trees. Nearer to the floor of the forest, numerous small deciduous and evergreen shrubs and trees will have flourished, such as ferns and myrtles.

1. The vegetation types identified by the pollen and spore analysis are almost all known to have grown well in damp conditions

2. The anoxic nature of the humic coal layer shows the vegetation grew in saturated soil, which means that all pore space within the soil is filled with liquid. This is indicative of a boggy / mire type environment.

3. The lava flow that the coal layer and the wagon-wheel structures lie on is unconsolidated hyaloclastite (hydrated breccia), this forms when lava flows through damp environments.

The pine trees are the exception to the damp-environment rule. However, they are relatively sparse in this particular area, probably due to the damp conditions. Samples collected from the same rock beds 1.5km northeast of where the wagon wheels were found indicate a significant increase in the relative abundance of pines, as well as a marked decrease in Taxodium trees. The most likely explanation for this is that between the soil samples used for this project and the samples just mentioned (1.5km northeast) there is a significant change in elevation. The latter sample was taken up-slope from the former, further away from the water source, and thus growing in drier conditions. This explains the variation in vegetation, as pine trees prefer drier conditions and Taxodium grow well in damp conditions.

15.2 Mull T2 (Ardtun)

The deposits of the Ardtun Leaf Beds (Sequence A6), provide an opportunity to compare the macroflora and palynoflora of alluvial-fluvial fan sequences in terms of botanical affinity, taphonomy and diversity. Comparison of the macrofossil and pollen and spore records for Ardtun reveals that the palynofloral record is 50% more diverse. This can be attributed to taphonomic factors, in particular the washing-in of pollen and spores from areas not contributing leaves to the macrofossil assemblage. Both the macrofossil and palynofloral data concur that *Ginkgo* occurred commonly on the alluvial fan surface. Substrate stability would have been an important factor in controlling the density and size of these shrubs or trees. However, it is the abundance of *Deltoidospora adriennis,* derived from a cyathacean fern, that demonstrates that ferns were the dominant taxon in a fern - *Ginkgo* scrub vegetation. Cyathacean or other fern fronds are not represented in the leaf beds, a factor we in part attribute to the adherent nature of the dead fern fronds on the plant. This factor would have been compounded by the ease of alluvial transportation of large volumes of cyathacean spores in contrast to the higher flow velocities needed to transport fern fronds into the site of preservation. Occuring as a part of this fern-*Ginkgo* community were producers of *Cupuliferoidaepollenites liblarensis* (Fagaceae) and *Triatriopollenites subtriangulus* (Myricaceae), possibly growing on better drained, relatively stable substrates within the alluvial fan. Members of the Cercidiphylaceae and Platanaceae are recorded as part of the leaf litter and as pollen, these plants constituting a small proportion of the vegetation. These taxa are associated with the margins of fluvial channels. Small areas of backswamp and saturated abandoned channels within the alluvial fan are suggested by the occurrence of Juglandaceae and Betulaceae fossils. The Juglandaceae are represented by macrofossils, and by *Momipites* pollen (Oreomunnioideae), but the *Alnus* type only by the pollen *Alnipollenites verus* and *A. trina.* The absence of betulaceous macrofossils at Ardtun can be attributed to the scarcity of these plants on the fan surface, as indicated by the low frequency of the pollen. In contrast, macrofossils of *Equisetum* are common as these plants were early successional colonists on unstable substrates in lava fields of the North Atlantic Igneous Province, including Mull (Boulter & Kvacek, 1989), where they form part of the streamside vegetation. Preservation of these fossil plants is not matched by their representation in the Ardtun palynoflora, their spores having a low preservation potential. We have recorded the contrasting macrofossil and spore records of cyathacean-type ferns at Ardtun. This contrast extends to other fern taxa, including the Osmundaceae which are absent as macrofossils, occurring commonly as *Baculatisporites primarius* spores. The distribution of Osmundacace in Arctic Paleogene vegetation (Basinger, 1991; McIver & Basinger, 1999), suggests that these ferns grew on dryer, recently exposed

substrates on the fan surface. In contrast to the record of Osmundaceae, a limited number of *Onoclea* fronds have been found in the leaf beds (Boulter & Kvacek, 1989). Spores attributed to the genus *Echinosporis* were suggested as being derived from these ferns by Boulter & Kvacek (1988), but these are not recorded at Ardtun. It is possible that instead the distribution of these *Onoclea* macrofossils can be compared to the occurrences of *Laevigatosporites haardtii* spores. These spores are thought to have been derived from a wide range of polypodiaceous ferns, including the Blechnaceae and Thelypteridaceae, (Collinson, 2002). Co-occurrences of *Trilites* species, *Dictyophylidites harisii* and *Gleicheniidites senonicus* spores with *L. haardtii* spores indicates that a part of the vegetation on the fan catchment was composed of these ferns. In Late Paleocene coal beds exposed on the Sagavanirktok River in Alaska and in the Early Eocene coals of the Faroe Islands Coal-bearing Formation (Ellis et al., 2002), *L. haardtii* producing ferns dominated the initial vegetation in newly established peat mires, a pattern of occurrence repeated here in the Mull Lava Field.

Although the leaves of taxodiaceous trees are recorded from Ardtun (Boulter & Kvacek, 1989), they are not common. This was contrasted by Boulter & Kvacek (1989) to the abundant occurrence of *Metasequoia* foliage in the late Palaeocene coals of Svalbard, and used to suggest that the lava field of Mull presented a habitat that was too disturbed by volcanism to support such vegetation. The palynoflora concurs, with only sparse occurrences of taxodiaceous pollen being recorded at Artun. However, this observation is at variance with data from other coeval sedimentary units within the North Atlantic Igneous Province (Jolley, 1997; Jolley et al.,2002; Ellis et al., 2002; Jolley & Whitham, 2004), and, as discussed below, within the Mull Lava Field itself. The low frequency of taxodiaceous pollen, which is derived from a group of trees known to be pollen over-producers indicates the absence of Taxodiaceae from the Ardtun alluvial fan. Localities in valley floor fluvial lithofacies to the north, and in coal swamp lithofacies to the south, both yeild considerable abundances of these pollen, indicating that floodplain and weathered lava flow top in the graben valley floor supported Taxodiaceae, whose pollen would have blown into the Ardtun fan site.

In summary, the Ardtun macrofossil and palynoflora assemblages indicate a fern - *Ginkgo* dominated vegetation, growing on comparatively well-drained soils. Ferns occurred sporadically, possibly concentrated in overbank marsh areas. Where the substrate became more stable, this fern marsh would have included trees or shrubs of the Platanaceae/Cercidiphylaceae, while in saturated mires Juglandaceae (*Momipites* producer) and Betulaceae (*Alnipollenites* producer) were commonly represented.

15.3 Svinair Section – Kvivik Beds – Malinstindur Formation

Due to the rapid eruption of high volumes of mafic compound lavas forming the lower part of the Malinstindur Formation, sedimentary deposits are largely absent. Above the distinctinve conglomerates and sandstones of the Kvivik Beds (Passey & Jolley, 2009) the Malinstindur Formation flows become thicker sheet lobes, and are separated by extensive interbeds indicating protracted weathering intervals between flows. This change reflects a slowing of the eruption tempo, and is critical to the understanding of the development of the Faroe Islands lava field, as it allows preservation of pollen and spores. One of the best examples of this interbed series

is preserved on the west coast of Esturoy between between Svinair and Eiði. While there are a succession of interbed units in this part of the Malinstindur Formation. Recently, Passey and Jolley (2010) have reported that the Kvívík Beds consist of laterally extensive deposits composed of volcaniclastic sandstones and conglomerates that generally lack well-developed sedimentary structures. They exhibit lateral transition from conglomerates to sandstones over vast areas in a manner comparable to facies transitions reported for mass flow deposits of volcanic and non-volcanic settings. Mass flows observed in ancient volcanic settings are generally inferred to have been deposited from rapidly flowing mixtures of debris and water (other than normal streamflow) originating from a volcano. Mass flows are essentially flood events involving a variety of different flow processes covering a wide spectrum of sediment/water ratios. They differ from their non-volcanic counterparts by lacking a significant clay content leading to non-cohesive flows that can travel significant distances exceeding 100 km from the source. To initiate a mass flow there needs to be an abundance of loose debris and water. The Kvívík Beds are composed almost exclusively of reworked pyroclastic debris supplied to the land surface by preceding (maybe many years) and/or contemporaneous volcanic activity. Water maybe released during and between volcanic eruptions and it is difficult, if not impossible, to identify the source of the water in ancient deposits. The most common sources are the ejection of crater-lake water, debris saturation by prolonged, periodically heavy, rainfall and breakouts from transient lakes dammed by previous mass flow deposits or even lava flows.

The volcaniclastic sandstones of the Kvívík Beds are interpreted as hyperconcentrated flows based on their horizontal bedding and fining upwards units. These sandstones have also been observed to mantle to palaeo-topography that is a common feature associated debris and hyperconcentrated flows travelling at high velocities. The sandstones do however commonly exhibit cross-bedding in their upper parts and locally thick cross-bedded sandstones are preserved. The presence of the cross-bedding suggests that these units were deposited under normal streamflow conditions, most likely, in braided river systems. This implies that either the hyperconcentrated flows became diluted downstream or they were subsequently reworked following initial deposition. The concentration of the thickest accumulations of the Kvívík Beds, most notably the volcaniclastic conglomerates, in the NW-SE corridor suggests that this area was a palaeo-low and the focus for deposition. The conglomerates, may therefore, be considered as valley-fills whereas the <2 m thick sandstones blanket the surrounding, albeit, low-lying floodplain. The prograding nature of the conglomerate lobes suggests that the palaeo-flow direction was to the S and based on the axial trend of the corridor was, most likely, to the SE. The Kvívík Beds most likely represent medial deposits between proximal deposits situated to the NW of the islands and distal deposits located to the SE. The proximal deposits may be derived from debris avalanches formed from the sector collapse of a volcanic edifice, but this is precluded by the lack of country rock debris (e.g. basalt lava flow clasts), brecciated clasts and significantly large (>10 m across) brecciated megaclasts in the volcaniclastic conglomerates. This also suggests that the mass flows, most likely, originated from breakouts of transient lakes associated with prolonged rainfall that washed additional pyroclastic material into the lakes and mass flows.

Preserved in these Kvivik Beds sediments are low diversity palynofloras. These palynofloras are best preserved in the sections exposed along the west side of Esturoy from Eiði and Svinoy. These sediments contain Inaperturopollenites hiatus *(*Glyptostrobus/Metasequoia*)* -dominated floras, some with common occurrences of Cupuliferoipollenites cingulum subspecies *(Fagaceae), Caryapollenites circulus (Juglandaceae)* and Deltoidospora adriennis *(cyathacean tree fern*). This assemblage is suggestive of weathered flow tops with base rich poorly drained soils supporting a pre-dominantly taxodiaceous vegetation, similar to mid successional communities recorded from older Faroese sediments.

15.3 Nes-Aeduvik: Argir Beds Enni Formation

The Argir Beds are dominated by volcaniclastic sandstones composed of palagonitised basaltic glass fragments. The beds are very similar texturally and compositionally in the exposures between Stóra Dímun and Eystnes peninsula, where the beds can be crudely separated into a lower, dominantly greenish clay-rich sandstone section and an upper, reddish brown clay-poor sandstone section (Jolley & Passey, 2010). A hiatus between the two sections is supported by the exposures around the Streymnev peninsula, Sandoy, where a flow lobe is observed to separate the lower and upper sections. The separation becomes more pronounced as the flow lobe thickens to >4 m in an easterly direction.

The lower, greenish clay-rich sandstones are generally structureless except for the development of weak, discontinuous sub-horizontal laminations. This lamination is clearly picked out by thin, <1 cm thick, laterally persistent, yellowish fine grained sands, interpreted to be primary volcaniclastic units – airfall tuffs. This contrasts with the upper, clay-poor sandstones that are characterised by scours/small-scale channels and broad, low-relief channels, several metres wide by a few decimetres deep. The exposure between Nes and Aeduvik shows a succession of coarse sandstones in fining upwards erosional channels. Primarily because of the grain-size, recovery of palynomorphs from this outcrop is poor, comprising fungal spores and the freshwater alage *Botryococcus braunii*. In some coeval locations such as those in the Torshavn area palynomorphs are recovered. The most commonly occurring species are *Inaperturopollenites hiatus* together with rare *Pityosporites spp.* , *Plicapollis pseudoexcelsus* and *Tricolpites* cf. *hians*. This pollen flora is derived from streamside vegetation dominated by Fagaceae (ashes) and Platanaceae (plane types), with the surrounding weathered flow top vegetated by a *Glyptostrobus/Metasequoia* woodland (swamp cypresses). The presence of fungal spores and *Botryococcus* at Nes suggests mass transport of rotting vegetation and the presence of small, probably ephemeral lakes.

16. GC-MS investigation

16.1 Extraction and fractionation

Samples were crushed in an agate pestle and mortar. Crusted samples (~7g) where spiked with recovery standards (squalane and 1,1'-binaphthyl) and then solvent extracted by Soxhlet using a dichloromethane:methanol mixture (DCM:MeOH; 93:7) for 24 hrs. Extracts were reduced in volume by rotary evaporation and under a stream of dry nitrogen. An apolar fraction was isolated by eluting the extract down a Florosil® solid phase extraction cartridge (500 mg, 3 ml) with 4 ml of DCM:hexane (1:1). This apolar fraction was then analysed by gas chromatography-mass spectrometry (GC-MS).

16.2 GC-MS analysis

GC-MS analysis was carried out using an Agilent Technologies 6890 gas chromatograph coupled to a 5973 mass spectrometer. Separation was performed on a J & W DB-5 column (30 m length, 0.25 mm internal diameter and 0.25 μm film thickness) with a He carrier gas at a constant column flow rate of 1.1 ml min^{-1}. The GC oven temperature was held for 1 min at 50 °C and ramped to 310 °C at a rate of 5 °C min^{-1} and then held for 9 min, injection was splitless at 270 °C.

16.3 Results

All the samples analysed contain low levels of extractable organics. The sediment samples do contain indigenous organic compounds, however in all but a couple of samples the most prominent components can be contributed to contamination most probably from the plastic samples bags used. Contaminates identified include phthalate esters, alkylbenzenes, diisopropylnaphthalenes, *tert*-butylated hydroxy toluenes, alkenes and normal and branched alkanes (cf. Grosjean et al., 2007; George et al., 2010). All the detected organic compounds in the lava samples can be attributed as being contaminants.

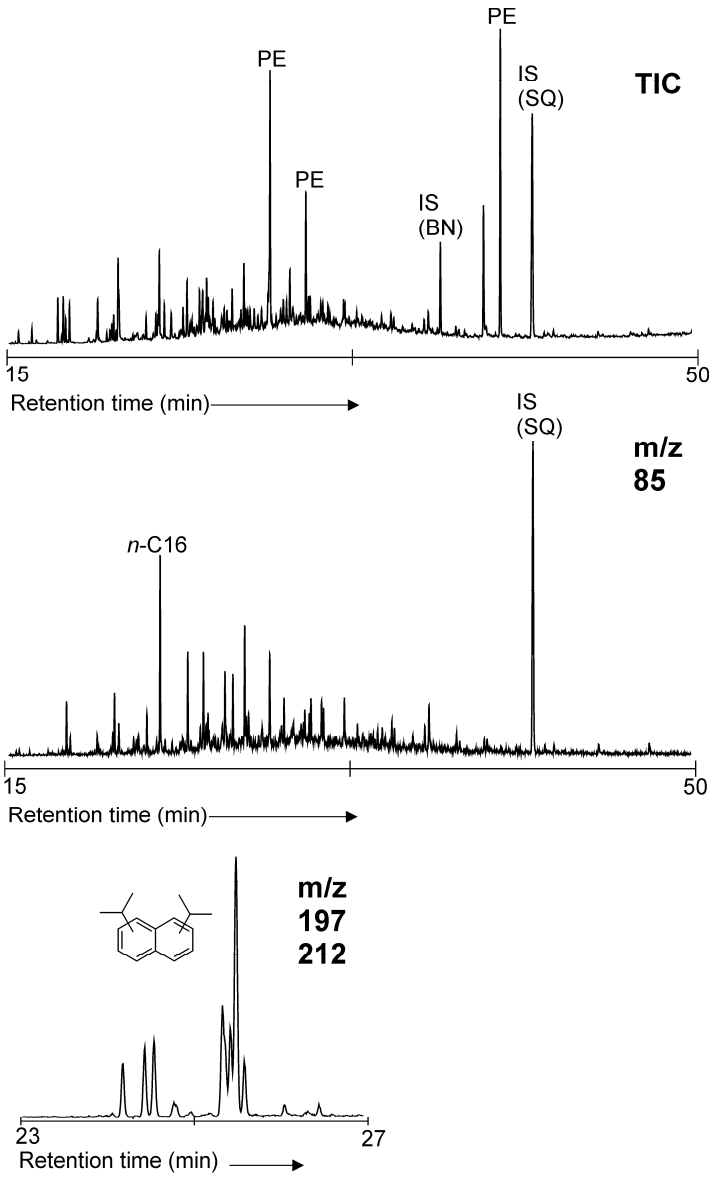

Figure 18: Sample F63, total ion chromatogram (TIC), partial mass chromatogram (*m/z* 85) displaying normal and branched alkanes and partially reconstructed chromatogram (*m/z* 197 + 212) displaying diisopropylnapthalenes. IS = internal standard, SQ = squalane, BN = 1,1'-binaphthyl, PE = phthalate ester.

17 Comparison of the Ar/Ar traverse data and reference to the model derived for the Mull T1 and T2 data

There are some striking similarities between some of the traverses and this can be related to the environments of lava emplacement.

a

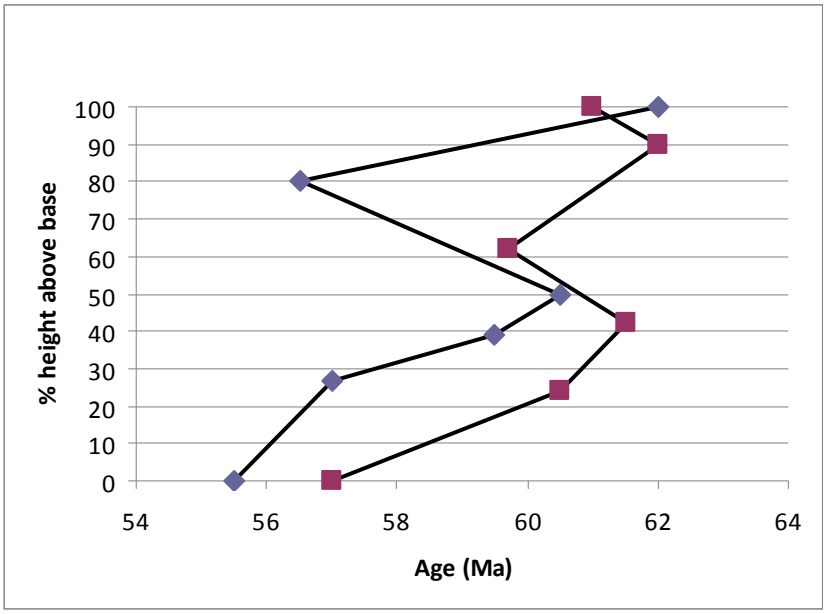

b

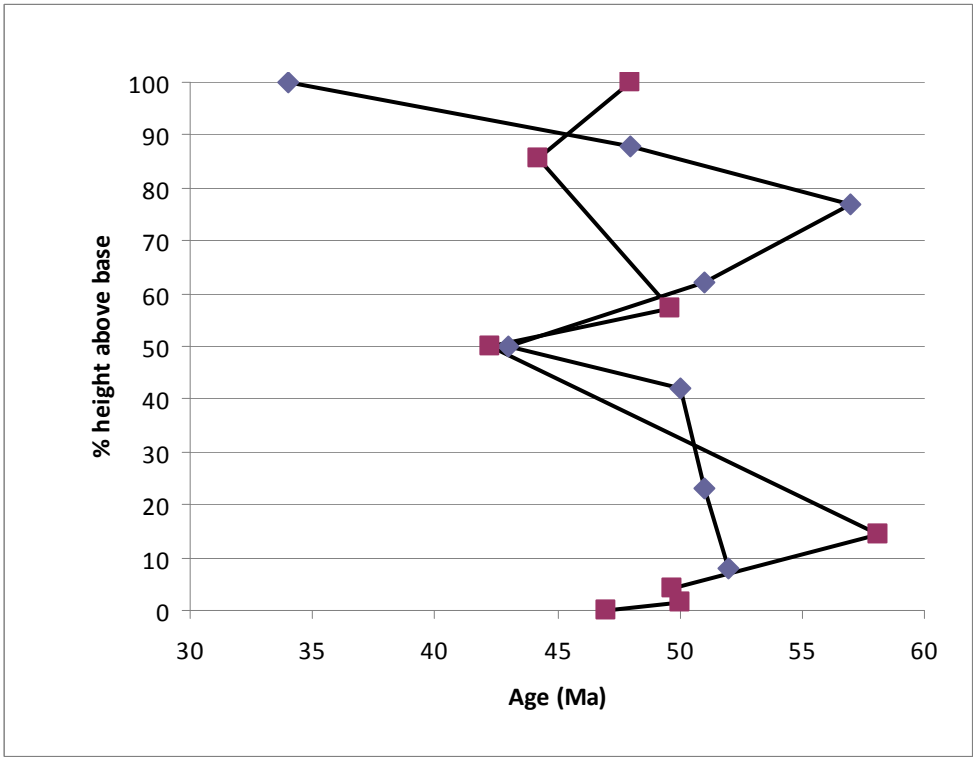

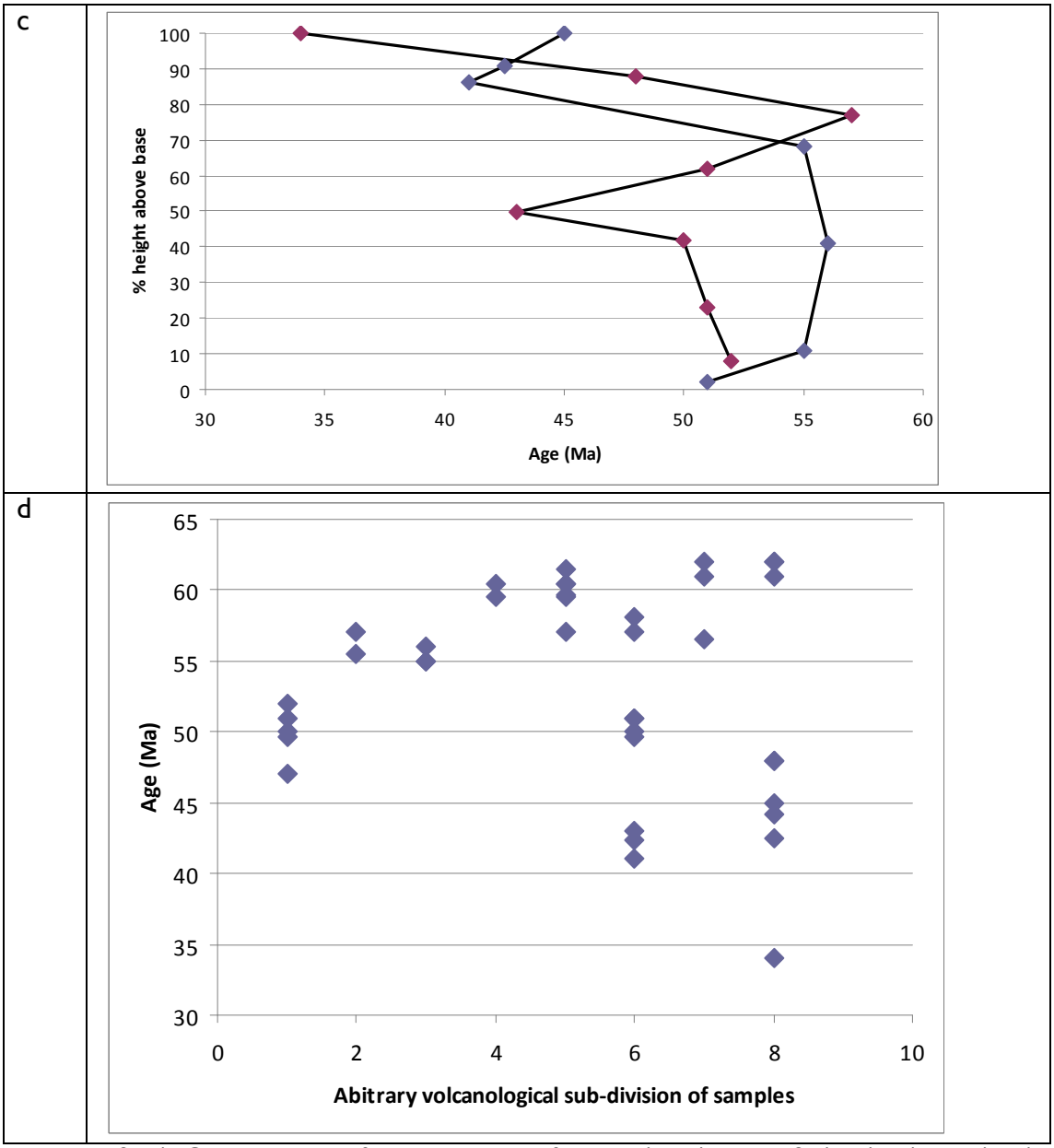

Figure 19. a) Comparison of age traverses for T1 (blue) and T2 (red); b) T5 (red) and T4 (blue); c) T5 (blue) and T3 (red); c) age versus 'arbitrary' volcanological sub-division: 1= base breccia, 2=pillowed base, 3=hyaloclastite, 4=massive core, 5=column, 6='non columnar' lava middle sections, 7=entablature, 8=lava tops.

Figure 19a is a reproduction of Figure 5, T1 and T2 from Mull, as discussed in earlier sections. Figure 19b compares T4 and T6, both very similar in that the two lavas are emplaced on thin fluvial volcanoclastic sands indicative of shallow water. The age profiles up the lava are similar, although the very base of T6 is missing the lowermost sample is giving an age within error of 55 Ma. Notably these two lavas are from two different formations – Malinstindur Formation (T4) and Enni Formatin (T6). Figure 19c compares the two traverses from Svinair Quarry in the Malinstindur Formation. The bases are within error of one another and 55 Ma but notably T4 from the northern end of the quarry preserves ages within error of 55 Ma within the bulk of the lava. Field evidence identifies that this part of the lava is brecciated and is associated with a deeper body of standing water than is T5 at the southern end of

the quarry. Figure 19d is a compilation of all data from Mull and the FIBG and broadly subdivided into 'volcanological' type. The breccia refers to the thin 'microbrecciation' observed at the bases of the lavas emplaced upon thin fluvial sands, whilst 'hyaloclastite' refers to the more massive brecciation as is observed in T4. The most reliable in terms of producing ages that are within error of the 55 Ma palynological ages for these lavas is the lava bases that have either hyaloclastite or pillows. These imply larger bodies of water and so a higher cooling rate on emplacement. Notably the cores of lavas, whether massive or colonnade, and entablatures and lava tops rarely if ever record the age of eruption when compared with palynological data, the ages frequently older. Drawing attention to the model derived for T1 and T2 the same model applies to the lavas in the FIBG – it is cooling rate and migration of 'excess argon' to the lava cores that is controlling the age variation observed in the lavas.

18. Conclusions

- There is no grain size control of Ar/Ar signature which simplifies the preparation procedure
- Lavas are strongly heterogeneous in terms of their Ar/Ar age signature relating to the presence of excess argon in the lavas
- The base of the lava yields ages that are the most accurate with regard to palynological ages and regional correlation
- The core of the lava is not appropriate for sample selection for Ar/Ar dating.
- The Ar/Ar age variation can be interpreted in the context of lava cooling rate – the highest cooling rate = most accurate ages, the lowest cooling rate = concentration of excess argon and elevated ages
- Ar/Ar ages from lava tops are complicated by weathering and leaching processes.
- Excess argon has been brought about by at least two processes: i) with alteration products, that outgas at low temperature; ii) inherent within the lava.
- The excess argon inherent in the lava could be derived from in situ decay of K and an inability for this component to 'escape' the lava, which is corroborated by the K_2O variations.
- The excess argon inherent in the lava could be derived from the original magma chamber, and not degassed on eruption.
- Published Ar/Ar ages for Mull are too old, and since Mull is considered correlative with the other Phase 1 volcanic centres (Skye, Small Isles, Antrim), it calls into question the dating of these centre.
- The same phenomena observed in Mull is also observed in the FIBG – Ar/Ar ages strongly controlled by rate of cooling which is determined by the presence and extent of standing water during eruption.
- The published ages for the Malinstindur and Enni Formation are likely to be too old, it is apparent from the new data here that the lava bases are within error of 55 Ma.
- Using published Ar/Ar ages from the NAIP to construct eruption rates is problematic.

19. Acknowledgements: I would like to thank the Sindri MC for permission to present the results at the Faroe Island Exploration Conference in Torshavn in September 2009, and for the opportunity to present the project at the Sindri MC Meeting. I would like to thank Simon Passey very much for field and logistical support.

20. Full references

Berggren WA et al 1995. A revised Cenozoic geochronology and chronostratigraphy, time scales and global stratigraphic correlations. Special Publication – Society for Sedimentary Geology, 129-212.

Chambers LM 2000 Age and duration of the British Tertiary igneous province. Implications for the development of the ancestral Iceland plume. PhD thesis, University of Edinburgh.

Chambers LM & MS Pringle 2001. Age and duration of activity at the Isle of Mull Tertiary igneous centre, Scotland, and confirmation of the existence of subchrons during Anomaly 26r. Earth and Planetary Science Letters, 193, 333-345.

Chambers LM et al 2005. Rapid formation of the Small Isles Tertiary centre constrained by precise Ar/Ar and U-Pb ages. Lithos, 79, 367-384.

Gamble J et al 1999. Constraints on the age of the British Tertiary Volcanic Province from ion microprobe U-Pb SHRIMP ages for acid igneous rocks from NE Ireland. Journal of the Geological Society 156, 291-299.

Ganerød M et al 2008. Reassembling the Paleogene-Eocene North Atlantic igneous province: New paleomagnetic constraints from the Isle of Mull, Scotland. Earth and Planetary Science Letters, 272, 464-475.

George, S.C., Volk, H., Romero-Sarmiento, M.-F., Dutiewicz, A., Mossman, D.J., 2010. Diisopropyl naphthalenes: Environmental contaminants of increasing importance for organic geochemical studies. Organic Geochemistry 41, 901-904.

Grosjean, E., Logan, G.A., 2007. Incorporation of organic contaminants into geochemical samples and an assessment of potential sources: Examples from Geoscience Australia marine survey S282. Organic Geochemistry 38, 853-869.

Jolley DW 1997. Palaeosurface palynofloras of the Skye lava field and the age of the British Tertiary Igneous Province. In: Widdowson M (Ed) Palaeosurfaces: recognition, reconstruction and palaeoenvironmental interpretation. Special Publication 120, Geological Society of London, 67-94.
Lyle P. 2000. The eruption environment of multi-tiered columnar basalt lava flows. Journal of the Geological Society of London, 157, 715-722.

Renne. P.R. et al., 1998. Intercalibration of standards, absolute ages and uncertainties in Ar/Ar dating. Chemical Geology, 145(1-2): 117-152.

Saunders A et al 1997. The North Atlantic Igneous Province. In: Mahoney JJ, Coffin MF (Eds), Large Igneous Provinces: Continental, Oceanic and Planetary flood basalt volcanism, AGU Monograph. American Geophysical Union 45-94.

Sherlock SC & Kelley SP 2002. Excess argon evolution in HP-LT rocks: a UVLAMP study of phengite and K-free minerals, NW Turkey. Chemical Geology, 182, 619-636.

White N & Lovell B 1997. Measuring the pulse of a plume with the sedimentary record. Nature 387, 6636, 888-891.

20. Appendices

20.1. Ar/Ar age data for T1

Sample	Step	^{40}Ar	±	^{39}Ar	±	^{38}Ar	±	^{37}Ar	±	^{36}Ar	±	^{40}Ar*/^{39}Ar	±	Age	±	^{39}Ar/^{40}Ar	±	^{36}Ar/^{40}Ar	±
B4	1	0.7462	0.0007	0.1561	0.0005	0.0018	0.0000	0.3196	0.0001	0.0002	0.0000	4.375	0.040	66.26	0.59	0.2092	0.0007	0.0003	0.0000
B4	2	0.2851	0.0007	0.0693	0.0001	0.0009	0.0000	0.1190	0.0001	0.0000	0.0000	4.212	0.085	63.83	1.26	0.2430	0.0008	-0.0001	-0.0001
B4	3	0.1471	0.0005	0.0360	0.0001	0.0004	0.0000	0.1671	0.0001	0.0000	0.0000	3.718	0.162	56.46	2.42	0.2449	0.0010	0.0003	0.0001
B4	4	0.0919	0.0005	0.0241	0.0001	0.0004	0.0000	0.1404	0.0001	0.0000	0.0000	3.678	0.242	55.86	3.63	0.2618	0.0016	0.0001	0.0002
B4	5	0.1333	0.0006	0.0338	0.0001	0.0004	0.0000	0.2387	0.0001	0.0001	0.0000	3.460	0.173	52.60	2.60	0.2534	0.0015	0.0004	0.0001
B4	6	0.0881	0.0006	0.0224	0.0001	0.0003	0.0000	0.1769	0.0001	0.0000	0.0000	3.907	0.260	59.29	3.89	0.2543	0.0017	0.0000	0.0002
B5	1	0.3550	0.0008	0.0272	0.0001	0.0004	0.0001	0.0602	0.0006	0.0005	0.0001	7.362	0.662	110.13	9.61	0.0766	0.0003	0.0015	0.0002
B5	2	0.5887	0.0021	0.0753	0.0006	0.0012	0.0001	0.1664	0.0006	0.0006	0.0001	5.638	0.244	84.93	3.59	0.1279	0.0011	0.0009	0.0001
B5	3	0.3981	0.0006	0.0662	0.0002	0.0009	0.0001	0.1480	0.0006	0.0003	0.0001	4.718	0.272	71.34	4.03	0.1662	0.0005	0.0007	0.0002
B5	4	0.8077	0.0014	0.1534	0.0004	0.0020	0.0001	0.3526	0.0006	0.0004	0.0001	4.577	0.118	69.26	1.75	0.1900	0.0006	0.0004	0.0001
B5	5	0.5790	0.0007	0.1097	0.0005	0.0015	0.0000	0.2659	0.0012	0.0003	0.0000	4.515	0.090	68.33	1.34	0.1895	0.0009	0.0005	0.0001
B5	6	0.4339	0.0011	0.0942	0.0003	0.0013	0.0000	0.2890	0.0012	0.0001	0.0000	4.239	0.104	64.24	1.55	0.2171	0.0010	0.0003	0.0001
B5	7	0.2653	0.0007	0.0620	0.0002	0.0008	0.0000	0.1910	0.0012	0.0001	0.0000	4.025	0.156	61.04	2.32	0.2338	0.0011	0.0002	0.0001
B5	8	0.3387	0.0005	0.0802	0.0002	0.0010	0.0000	0.4071	0.0012	0.0001	0.0000	3.834	0.120	58.19	1.80	0.2368	0.0008	0.0003	0.0001
B5	9	0.1431	0.0004	0.0352	0.0002	0.0004	0.0000	0.1650	0.0012	0.0001	0.0000	3.483	0.274	52.94	4.10	0.2458	0.0015	0.0005	0.0002
B5	10	0.1422	0.0005	0.0368	0.0002	0.0003	0.0000	0.1865	0.0012	0.0000	0.0000	3.674	0.262	55.80	3.92	0.2587	0.0016	0.0002	0.0002
B6	1	0.4448	0.0007	0.0272	0.0001	0.0006	0.0001	0.1146	0.0001	0.0011	0.0000	4.802	0.401	72.58	5.94	0.0612	0.0002	0.0024	0.0001
B6	2	0.3507	0.0010	0.0436	0.0001	0.0006	0.0001	0.0798	0.0001	0.0006	0.0000	4.303	0.251	65.18	3.73	0.1243	0.0004	0.0016	0.0001
B6	3	0.3528	0.0007	0.0686	0.0001	0.0007	0.0000	0.1400	0.0001	0.0002	0.0000	4.127	0.140	62.56	2.09	0.1944	0.0005	0.0007	0.0001
B6	4	0.2117	0.0007	0.0429	0.0001	0.0006	0.0000	0.1299	0.0001	0.0002	0.0000	3.775	0.225	57.31	3.36	0.2024	0.0009	0.0008	0.0002
B6	5	0.2674	0.0007	0.0595	0.0001	0.0010	0.0001	0.3195	0.0001	0.0001	0.0000	3.758	0.162	57.05	2.42	0.2224	0.0007	0.0006	0.0001
B6	6	0.1174	0.0008	0.0246	0.0001	0.0003	0.0001	0.1455	0.0001	0.0001	0.0000	3.279	0.392	49.88	5.89	0.2092	0.0016	0.0011	0.0003
B6	7	0.1412	0.0006	0.0313	0.0001	0.0003	0.0000	0.2145	0.0001	0.0001	0.0000	3.972	0.307	60.26	4.59	0.2220	0.0013	0.0004	0.0002

Sample	Step	^{40}Ar	±	^{39}Ar	±	^{38}Ar	±	^{37}Ar	±	^{36}Ar	±	$^{40}Ar^*/^{39}Ar$	±	Age	±	$^{39}Ar/^{40}Ar$	±	$^{36}Ar/^{40}Ar$	±
B7	1	0.5357	0.0006	0.0125	0.0001	0.0005	0.0000	0.0264	0.0001	0.0015	0.0000	7.784	0.697	116.24	10.09	0.0234	0.0001	0.0028	0.0001
B7	2	0.3491	0.0009	0.0226	0.0001	0.0003	0.0000	0.0520	0.0001	0.0008	0.0000	4.900	0.315	74.04	4.67	0.0648	0.0004	0.0023	0.0001
B7	3	0.4673	0.0006	0.0442	0.0001	0.0008	0.0000	0.1056	0.0001	0.0007	0.0000	5.685	0.198	85.62	2.91	0.0945	0.0003	0.0016	0.0001
B7	4	0.4393	0.0005	0.0519	0.0001	0.0007	0.0000	0.1339	0.0001	0.0006	0.0000	5.018	0.136	75.78	2.02	0.1182	0.0003	0.0014	0.0001
B7	5	0.3470	0.0007	0.0597	0.0002	0.0007	0.0000	0.1362	0.0001	0.0002	0.0000	4.652	0.147	70.37	2.18	0.1721	0.0006	0.0007	0.0001
B7	6	0.4968	0.0008	0.0997	0.0001	0.0013	0.0000	0.2417	0.0001	0.0003	0.0000	4.104	0.071	62.22	1.06	0.2007	0.0004	0.0006	0.0000
B7	7	0.2939	0.0005	0.0626	0.0002	0.0008	0.0000	0.2023	0.0001	0.0002	0.0000	3.957	0.113	60.03	1.69	0.2130	0.0006	0.0005	0.0001
B7	8	0.3502	0.0004	0.0744	0.0001	0.0010	0.0000	0.2665	0.0001	0.0002	0.0000	3.953	0.095	59.97	1.42	0.2125	0.0004	0.0005	0.0001
B7	9	0.4471	0.0005	0.0936	0.0001	0.0011	0.0000	0.4581	0.0001	0.0003	0.0000	3.898	0.076	59.15	1.13	0.2093	0.0004	0.0006	0.0001
B8	1	0.6939	0.0005	0.0133	0.0001	0.0005	0.0000	0.0284	0.0002	0.0022	0.0000	3.466	0.760	52.69	11.38	0.0191	0.0001	0.0032	0.0000
B8	2	0.8278	0.0009	0.0379	0.0001	0.0010	0.0000	0.0907	0.0002	0.0024	0.0000	3.238	0.230	49.27	3.45	0.0458	0.0001	0.0029	0.0000
B8	3	0.5590	0.0012	0.0488	0.0002	0.0009	0.0000	0.1354	0.0002	0.0011	0.0000	4.652	0.180	70.36	2.67	0.0872	0.0004	0.0020	0.0001
B8	4	0.6467	0.0007	0.0860	0.0001	0.0013	0.0000	0.2630	0.0002	0.0011	0.0000	3.668	0.101	55.71	1.51	0.1331	0.0003	0.0017	0.0000
B8	5	0.6547	0.0015	0.1063	0.0002	0.0014	0.0000	0.3858	0.0002	0.0009	0.0000	3.664	0.096	55.64	1.44	0.1623	0.0005	0.0014	0.0001
B8	6	0.3382	0.0010	0.0621	0.0002	0.0009	0.0000	0.2383	0.0002	0.0004	0.0000	3.746	0.141	56.87	2.10	0.1837	0.0007	0.0011	0.0001
B8	7	0.4223	0.0007	0.0698	0.0001	0.0012	0.0000	0.3194	0.0002	0.0005	0.0000	3.869	0.145	58.72	2.16	0.1653	0.0003	0.0012	0.0001
B8	8	0.2280	0.0005	0.0387	0.0001	0.0006	0.0000	0.2104	0.0002	0.0003	0.0000	3.266	0.225	49.69	3.37	0.1696	0.0006	0.0015	0.0001
B8	9	0.5855	0.0028	0.1027	0.0005	0.0015	0.0000	0.5996	0.0002	0.0006	0.0000	3.856	0.091	58.52	1.35	0.1754	0.0012	0.0011	0.0001
B9	1	0.1490	0.0006	0.0194	0.0001	0.0003	0.0000	0.0360	0.0002	0.0001	0.0000	5.579	0.525	84.07	7.73	0.1305	0.0007	0.0009	0.0002
B9	2	0.1614	0.0002	0.0284	0.0001	0.0002	0.0000	0.0416	0.0002	0.0001	0.0000	4.891	0.359	73.90	5.31	0.1762	0.0007	0.0005	0.0002
B9	3	0.2517	0.0005	0.0526	0.0001	0.0006	0.0000	0.0634	0.0002	0.0000	0.0000	4.508	0.194	68.23	2.88	0.2088	0.0006	0.0002	0.0001
B9	4	0.2880	0.0009	0.0625	0.0001	0.0008	0.0000	0.0704	0.0002	0.0001	0.0000	4.193	0.164	63.55	2.44	0.2169	0.0007	0.0003	0.0001
B9	5	0.2449	0.0003	0.0578	0.0001	0.0007	0.0000	0.0647	0.0002	0.0000	0.0000	4.034	0.177	61.17	2.63	0.2361	0.0007	0.0002	0.0001
B9	6	0.3315	0.0003	0.0791	0.0001	0.0010	0.0000	0.1165	0.0002	0.0000	0.0000	4.205	0.129	63.73	1.92	0.2387	0.0005	0.0000	-0.0001
B9	7	0.2321	0.0003	0.0567	0.0001	0.0007	0.0000	0.1519	0.0002	0.0000	0.0000	4.219	0.180	63.93	2.68	0.2441	0.0006	-0.0001	-0.0001
B9	8	0.1479	0.0002	0.0375	0.0001	0.0005	0.0000	0.1512	0.0002	0.0000	0.0000	3.810	0.272	57.84	4.06	0.2537	0.0006	0.0001	0.0002
B9	9	0.0830	0.0003	0.0206	0.0000	0.0003	0.0000	0.0872	0.0002	0.0000	0.0000	3.826	0.494	58.07	7.38	0.2487	0.0009	0.0002	0.0004
B9	10	0.2931	0.0007	0.0728	0.0003	0.0009	0.0000	0.6550	0.0002	0.0000	0.0000	3.852	0.141	58.46	2.11	0.2483	0.0011	0.0001	0.0001

20.2. Ar/Ar age data for T2

Sample	Step	^{40}Ar	±	^{39}Ar	±	^{38}Ar	±	^{37}Ar	±	^{36}Ar	±	^{40}Ar*/^{39}Ar	±	Age	±	^{39}Ar/^{40}Ar	±	^{36}Ar/^{40}Ar	±
A46	1	0.4145	0.0003	0.0707	0.0001	0.0010	0.0000	0.1983	0.0001	0.0004	0.0000	4.100	0.063	62.16	0.94	0.1705	0.0003	0.0010	0.0000
A46	2	0.4024	0.0007	0.0902	0.0001	0.0011	0.0000	0.1785	0.0001	0.0002	0.0000	3.845	0.050	58.36	0.75	0.2242	0.0005	0.0005	0.0000
A46	3	0.3304	0.0005	0.0799	0.0002	0.0010	0.0000	0.1581	0.0001	0.0001	0.0000	3.645	0.057	55.37	0.85	0.2417	0.0008	0.0004	0.0000
A46	4	0.2160	0.0006	0.0525	0.0002	0.0007	0.0000	0.1427	0.0001	0.0000	0.0000	3.903	0.087	59.23	1.29	0.2432	0.0012	0.0002	0.0001
A46	5	0.2302	0.0014	0.0579	0.0002	0.0006	0.0000	0.2066	0.0001	0.0000	0.0000	3.820	0.081	57.99	1.22	0.2516	0.0018	0.0001	0.0001
A46	6	0.2233	0.0004	0.0537	0.0001	0.0005	0.0000	0.2879	0.0001	0.0001	0.0000	3.723	0.083	56.53	1.25	0.2406	0.0008	0.0004	0.0001
A46	7	0.2076	0.0010	0.0521	0.0003	0.0007	0.0000	0.2511	0.0001	0.0001	0.0000	3.655	0.089	55.52	1.34	0.2508	0.0018	0.0003	0.0001
A46	8	0.1571	0.0004	0.0376	0.0001	0.0005	0.0000	0.2132	0.0001	0.0000	0.0000	3.798	0.118	57.65	1.77	0.2393	0.0007	0.0003	0.0001
A47	1	0.4192	0.0009	0.0648	0.0001	0.0009	0.0000	0.2354	0.0001	0.0005	0.0000	4.357	0.070	65.98	1.04	0.1547	0.0004	0.0011	0.0000
A47	2	0.2981	0.0007	0.0609	0.0002	0.0008	0.0000	0.1929	0.0001	0.0002	0.0000	4.053	0.075	61.46	1.12	0.2042	0.0009	0.0006	0.0001
A47	3	0.3640	0.0015	0.0822	0.0002	0.0010	0.0000	0.2383	0.0001	0.0001	0.0000	3.991	0.058	60.54	0.86	0.2258	0.0011	0.0003	0.0000
A47	4	0.2075	0.0006	0.0482	0.0001	0.0006	0.0000	0.1569	0.0001	0.0000	0.0000	4.040	0.093	61.26	1.39	0.2322	0.0009	0.0002	0.0001
A47	5	0.1964	0.0006	0.0471	0.0001	0.0005	0.0000	0.1744	0.0001	0.0000	0.0000	3.864	0.096	58.64	1.43	0.2398	0.0010	0.0002	0.0001
A47	6	0.4048	0.0009	0.0987	0.0003	0.0014	0.0000	0.4433	0.0001	0.0000	0.0000	3.957	0.047	60.03	0.70	0.2439	0.0009	0.0001	0.0000
A48	1	0.7953	0.0021	0.1224	0.0003	0.0015	0.0000	0.3454	0.0001	0.0010	0.0000	4.074	0.041	61.77	0.62	0.1539	0.0006	0.0013	0.0000
A48	2	0.3903	0.0007	0.0811	0.0001	0.0010	0.0000	0.2240	0.0001	0.0001	0.0000	4.290	0.087	64.99	1.29	0.2077	0.0005	0.0004	0.0001
A48	3	0.3375	0.0004	0.0762	0.0004	0.0010	0.0000	0.2008	0.0001	0.0002	0.0000	3.809	0.094	57.82	1.40	0.2257	0.0012	0.0005	0.0001
A48	4	0.2428	0.0004	0.0568	0.0001	0.0007	0.0000	0.1898	0.0001	0.0000	0.0000	4.100	0.123	62.16	1.84	0.2341	0.0007	0.0001	0.0001
A48	5	0.1899	0.0004	0.0477	0.0002	0.0006	0.0000	0.2003	0.0001	0.0000	0.0000	3.860	0.147	58.59	2.20	0.2509	0.0011	0.0001	0.0001
A48	6	0.1352	0.0003	0.0341	0.0001	0.0004	0.0000	0.1553	0.0001	0.0000	0.0000	4.119	0.205	62.44	3.05	0.2522	0.0009	-0.0001	-0.0002

Sample	Step	^{40}Ar	±	^{39}Ar	±	^{38}Ar	±	^{37}Ar	±	^{36}Ar	±	$^{40}Ar^*/^{39}Ar$	±	Age	±	$^{39}Ar/^{40}Ar$	±	$^{36}Ar/^{40}Ar$	±
A49	1	0.5643	0.0011	0.1178	0.0002	0.0014	0.0000	0.2936	0.0001	0.0003	0.0000	3.973	0.060	60.26	0.90	0.2088	0.0005	0.0006	0.0000
A49	2	0.3809	0.0006	0.0944	0.0001	0.0010	0.0000	0.1526	0.0001	0.0000	0.0000	3.995	0.074	60.60	1.11	0.2478	0.0004	0.0000	0.0001
A49	3	0.2320	0.0004	0.0601	0.0001	0.0007	0.0000	0.1181	0.0001	0.0000	0.0000	3.753	0.116	56.99	1.74	0.2589	0.0007	0.0001	0.0001
A49	4	0.1908	0.0004	0.0488	0.0001	0.0006	0.0000	0.1788	0.0001	0.0000	0.0000	3.633	0.178	55.19	2.66	0.2556	0.0008	0.0002	0.0002
A49	5	0.1523	0.0003	0.0385	0.0002	0.0005	0.0000	0.2260	0.0001	0.0000	0.0000	4.079	0.182	61.85	2.71	0.2530	0.0011	-0.0001	-0.0002
A49	6	0.1989	0.0002	0.0495	0.0001	0.0006	0.0000	0.3447	0.0001	0.0000	0.0000	3.883	0.141	58.92	2.11	0.2491	0.0008	0.0001	0.0001
A50	1	0.5780	0.0007	0.0579	0.0001	0.0008	0.0000	0.1443	0.0001	0.0011	0.0000	4.568	0.101	69.13	1.50	0.1002	0.0002	0.0018	0.0000
A50	2	0.3824	0.0055	0.0724	0.0009	0.0008	0.0000	0.1451	0.0001	0.0003	0.0000	4.138	0.142	62.73	2.11	0.1893	0.0037	0.0007	0.0001
A50	3	0.2334	0.0007	0.0512	0.0001	0.0007	0.0000	0.0913	0.0001	0.0000	0.0000	4.298	0.114	65.11	1.70	0.2195	0.0007	0.0002	0.0001
A50	4	0.3183	0.0006	0.0728	0.0001	0.0008	0.0000	0.1210	0.0001	0.0001	0.0000	4.018	0.080	60.94	1.20	0.2288	0.0005	0.0003	0.0001
A50	5	0.2616	0.0005	0.0636	0.0001	0.0009	0.0000	0.1632	0.0001	0.0000	0.0000	3.902	0.092	59.20	1.37	0.2431	0.0006	0.0002	0.0001
A50	6	0.1897	0.0005	0.0456	0.0000	0.0007	0.0000	0.1614	0.0001	0.0000	0.0000	4.124	0.128	62.51	1.91	0.2403	0.0007	0.0000	0.0001
A50	7	0.2151	0.0007	0.0471	0.0001	0.0006	0.0000	0.2357	0.0001	0.0002	0.0000	3.522	0.124	53.52	1.86	0.2191	0.0008	0.0008	0.0001
A50	8	0.9013	0.0016	0.0397	0.0002	0.0010	0.0000	0.2364	0.0001	0.0025	0.0000	4.053	0.200	61.46	2.98	0.0440	0.0002	0.0028	0.0000
A52	1	0.5796	0.0006	0.0848	0.0003	0.0012	0.0000	0.2196	0.0005	0.0006	0.0000	4.774	0.083	72.18	1.23	0.1463	0.0005	0.0010	0.0000
A52	2	0.4235	0.0005	0.0690	0.0002	0.0010	0.0000	0.1703	0.0005	0.0004	0.0000	4.578	0.102	69.26	1.51	0.1628	0.0005	0.0009	0.0001
A52	3	1.8922	0.0061	0.1558	0.0006	0.0028	0.0000	0.3902	0.0005	0.0042	0.0000	4.262	0.070	64.58	1.04	0.0823	0.0004	0.0022	0.0000
A52	4	0.7185	0.0011	0.1334	0.0002	0.0017	0.0000	0.3756	0.0005	0.0005	0.0000	4.255	0.053	64.47	0.79	0.1857	0.0004	0.0007	0.0000
A52	5	0.8317	0.0008	0.1732	0.0002	0.0020	0.0000	0.4815	0.0005	0.0004	0.0000	4.082	0.041	61.89	0.60	0.2082	0.0003	0.0005	0.0000
A52	6	0.7867	0.0006	0.1828	0.0003	0.0022	0.0000	0.5794	0.0005	0.0002	0.0000	3.953	0.048	59.97	0.71	0.2324	0.0004	0.0003	0.0000
A52	7	0.5049	0.0007	0.1202	0.0002	0.0014	0.0000	0.3967	0.0005	0.0001	0.0000	3.870	0.058	58.73	0.87	0.2380	0.0006	0.0003	0.0000
A52	8	0.6378	0.0016	0.1475	0.0003	0.0018	0.0000	0.6742	0.0005	0.0002	0.0000	3.939	0.049	59.76	0.73	0.2314	0.0008	0.0003	0.0000
A52	9	0.4312	0.0005	0.1010	0.0002	0.0012	0.0000	0.5219	0.0005	0.0001	0.0000	4.089	0.069	61.99	1.03	0.2342	0.0005	0.0001	0.0001

20.3 Ar/Ar age data for T3

Sample	Step	^{40}Ar	±	^{39}Ar	±	^{38}Ar	±	^{37}Ar	±	^{36}Ar	±	$^{40}Ar^*/^{39}Ar$	±	Age	±	$^{39}Ar/^{40}Ar$	±	$^{36}Ar/^{40}Ar$	±
M41	1	0.1197	0.0009	0.0007	0.0001	0.0000	0.0000	0.0215	0.0006	0.0003	0.0000	56.93	18.49	776	205	0.0056	0.0005	0.0023	0.0003
M41	2	0.9500	0.0010	0.0060	0.0000	0.0007	0.0000	0.2056	0.0006	0.0030	0.0000	12.78	2.46	206	37	0.0063	0.0000	0.0031	0.0001
M41	3	2.2204	0.0016	0.0106	0.0000	0.0016	0.0000	0.3876	0.0006	0.0071	0.0000	10.43	1.24	170	19	0.0048	0.0000	0.0032	0.0000
M41	4	0.7657	0.0014	0.0117	0.0001	0.0006	0.0000	0.3713	0.0006	0.0023	0.0000	7.31	1.13	120	18	0.0152	0.0001	0.0030	0.0001
M41	5	0.4918	0.0008	0.0183	0.0001	0.0006	0.0000	0.4710	0.0006	0.0014	0.0000	4.82	0.72	80	12	0.0372	0.0001	0.0028	0.0001
M41	6	0.6167	0.0012	0.0218	0.0001	0.0006	0.0000	0.5252	0.0006	0.0017	0.0000	5.22	0.55	87	9	0.0353	0.0002	0.0028	0.0001
M41	7	0.5453	0.0007	0.0199	0.0001	0.0005	0.0000	0.4183	0.0006	0.0014	0.0000	7.21	0.66	119	11	0.0365	0.0002	0.0025	0.0001
M41	8	1.2087	0.0015	0.0395	0.0000	0.0010	0.0001	0.7457	0.0006	0.0034	0.0000	5.14	0.33	86	5	0.0326	0.0001	0.0028	0.0000
M42	1	0.0610	0.0007	0.0007	0.0001	0.0000	0.0000	0.0375	0.0004	0.0002	0.0000	-8.21	-16.72	-146	309	0.0119	0.0009	0.0037	0.0007
M42	2	0.4652	0.0010	0.0043	0.0001	0.0001	0.0001	0.2546	0.0004	0.0015	0.0000	5.85	2.84	97	46	0.0092	0.0001	0.0032	0.0001
M42	3	1.1640	0.0021	0.0087	0.0001	0.0010	0.0001	0.4022	0.0004	0.0041	0.0000	-4.80	-1.30	-84	23	0.0074	0.0001	0.0035	0.0000
M42	4	0.7080	0.0010	0.0086	0.0001	0.0006	0.0000	0.3712	0.0004	0.0023	0.0000	3.01	1.29	51	21	0.0122	0.0001	0.0033	0.0001
M42	5	0.4365	0.0008	0.0158	0.0002	0.0007	0.0001	0.5932	0.0004	0.0012	0.0000	4.63	0.70	77	11	0.0362	0.0004	0.0028	0.0001
M42	6	0.5109	0.0013	0.0205	0.0001	0.0006	0.0001	0.7367	0.0004	0.0014	0.0000	5.02	0.60	84	10	0.0401	0.0002	0.0027	0.0001
M42	7	0.3509	0.0011	0.0158	0.0001	0.0006	0.0000	0.5374	0.0009	0.0010	0.0000	4.01	0.65	67	11	0.0451	0.0003	0.0028	0.0001
M42	8	0.4710	0.0015	0.0254	0.0001	0.0005	0.0000	0.8111	0.0009	0.0013	0.0000	3.76	0.41	63	7	0.0540	0.0003	0.0027	0.0001

Sample	Step	^{40}Ar	±	^{39}Ar	±	^{38}Ar	±	^{37}Ar	±	^{36}Ar	±	$^{40}Ar^*/^{39}Ar$	±	Age	±	$^{39}Ar/^{40}Ar$	±	$^{36}Ar/^{40}Ar$	±
M43	1	0.1161	0.0011	0.0003	0.0000	0.0001	0.0001	0.0093	0.0003	0.0003	0.0001	70.18	54.50	920	560	0.0029	0.0004	0.0027	0.0005
M43	2	0.6938	0.0013	0.0028	0.0000	0.0005	0.0001	0.0801	0.0003	0.0022	0.0001	19.34	6.65	304	96	0.0040	0.0001	0.0031	0.0001
M43	3	3.7254	0.0024	0.0177	0.0001	0.0024	0.0001	0.3850	0.0003	0.0122	0.0001	6.04	1.20	100	19	0.0048	0.0000	0.0033	0.0000
M43	4	4.1748	0.0031	0.0305	0.0001	0.0033	0.0001	0.6568	0.0003	0.0139	0.0001	2.19	0.76	37	13	0.0073	0.0000	0.0033	0.0000
M43	5	1.7229	0.0031	0.0269	0.0002	0.0013	0.0001	0.8585	0.0007	0.0053	0.0001	5.93	0.60	99	10	0.0156	0.0001	0.0031	0.0000
M43	6	1.6366	0.0017	0.0360	0.0001	0.0015	0.0001	1.3532	0.0007	0.0048	0.0000	5.98	0.40	100	7	0.0220	0.0001	0.0029	0.0000
M43	7	1.6464	0.0020	0.0583	0.0002	0.0017	0.0001	2.1819	0.0007	0.0044	0.0000	5.99	0.25	100	4	0.0354	0.0001	0.0027	0.0000
M43	8	1.2211	0.0016	0.0548	0.0001	0.0013	0.0001	1.8105	0.0007	0.0029	0.0001	6.71	0.29	111	5	0.0449	0.0001	0.0024	0.0000
M43	9	0.3070	0.0016	0.0186	0.0001	0.0004	0.0001	0.4198	0.0007	0.0007	0.0000	5.28	0.78	88	13	0.0605	0.0004	0.0023	0.0002
M44	1	0.6011	0.0006	0.0076	0.0001	0.0006	0.0000	0.0508	0.0004	0.0018	0.0000	8.34	1.35	137	21	0.0127	0.0001	0.0030	0.0001
M44	2	0.6058	0.0008	0.0198	0.0001	0.0007	0.0000	0.1210	0.0004	0.0018	0.0000	4.31	0.52	72	9	0.0327	0.0001	0.0029	0.0001
M44	3	2.1222	0.0018	0.0792	0.0001	0.0023	0.0000	0.4431	0.0004	0.0060	0.0000	4.46	0.17	75	3	0.0373	0.0001	0.0028	0.0000
M44	4	1.2280	0.0019	0.0971	0.0003	0.0014	0.0001	0.6147	0.0004	0.0028	0.0000	4.13	0.12	69	2	0.0791	0.0003	0.0023	0.0000
M44	5	1.0435	0.0012	0.1207	0.0002	0.0017	0.0000	0.7193	0.0004	0.0017	0.0000	4.53	0.09	76	1	0.1157	0.0002	0.0016	0.0000
M44	6	1.1434	0.0009	0.1245	0.0001	0.0020	0.0000	0.7299	0.0004	0.0021	0.0000	4.25	0.09	71	2	0.1089	0.0001	0.0018	0.0000
M44	7	0.8644	0.0008	0.0776	0.0001	0.0013	0.0000	0.4847	0.0004	0.0019	0.0000	3.85	0.15	65	2	0.0898	0.0002	0.0022	0.0000
M44	8	1.0115	0.0009	0.0820	0.0002	0.0015	0.0000	0.5647	0.0004	0.0021	0.0000	4.86	0.14	81	2	0.0811	0.0002	0.0020	0.0000

20.4 Ar/Ar age data for T4

Sample	Step	^{40}Ar	±	^{39}Ar	±	^{38}Ar	±	^{37}Ar	±	^{36}Ar	±	^{40}Ar*/^{39}Ar	±	Age	±	^{39}Ar/^{40}Ar	±	^{36}Ar/^{40}Ar	±
F71	1	0.3389	0.0003	0.0016	0.0001	0.0002	0.0000	0.0409	0.0007	0.0011	0.0000	2.4	3.4	41	57	0.0046	0.0002	0.0033	0.0001
F71	2	0.8500	0.0007	0.0082	0.0001	0.0006	0.0000	0.1907	0.0007	0.0027	0.0000	5.1	0.9	86	15	0.0097	0.0001	0.0032	0.0000
F71	3	0.3992	0.0009	0.0109	0.0001	0.0003	0.0000	0.3047	0.0007	0.0012	0.0000	3.4	0.5	58	8	0.0274	0.0002	0.0031	0.0000
F71	4	0.3468	0.0004	0.0205	0.0001	0.0005	0.0000	0.7522	0.0007	0.0010	0.0000	3.0	0.3	51	4	0.0592	0.0002	0.0028	0.0001
F71	5	0.1952	0.0002	0.0147	0.0001	0.0003	0.0000	0.8627	0.0007	0.0005	0.0000	2.7	0.4	46	6	0.0755	0.0005	0.0027	0.0001
F71	6	0.2483	0.0007	0.0225	0.0001	0.0005	0.0000	1.6319	0.0007	0.0006	0.0000	2.9	0.2	49	4	0.0908	0.0004	0.0025	0.0001
F71	7	0.1352	0.0002	0.0120	0.0001	0.0002	0.0000	1.0380	0.0004	0.0003	0.0000	3.8	0.7	65	12	0.0891	0.0004	0.0022	0.0002
F71	8	0.1885	0.0003	0.0186	0.0000	0.0003	0.0000	1.6805	0.0004	0.0005	0.0000	2.8	0.4	48	6	0.0987	0.0003	0.0025	0.0001
F72	1	0.3223	0.0006	0.0024	0.0000	0.0002	0.0000	0.0247	0.0003	0.0010	0.0000	10.6	3.9	173	61	0.0074	0.0001	0.0031	0.0001
F72	2	0.7207	0.0018	0.0069	0.0001	0.0004	0.0000	0.0926	0.0003	0.0023	0.0000	7.7	1.6	128	25	0.0096	0.0001	0.0031	0.0001
F72	3	0.7257	0.0008	0.0138	0.0001	0.0006	0.0000	0.2564	0.0003	0.0021	0.0000	7.3	0.7	121	11	0.0191	0.0001	0.0029	0.0000
F72	4	0.3685	0.0004	0.0173	0.0001	0.0004	0.0000	0.4580	0.0003	0.0010	0.0000	4.0	0.5	68	9	0.0470	0.0003	0.0027	0.0001
F72	5	0.2993	0.0002	0.0234	0.0001	0.0003	0.0000	0.8674	0.0004	0.0007	0.0000	4.6	0.5	76	7	0.0782	0.0002	0.0022	0.0001
F72	6	0.2343	0.0002	0.0246	0.0001	0.0004	0.0000	1.1543	0.0004	0.0005	0.0000	3.6	0.4	60	6	0.1051	0.0004	0.0021	0.0001
F72	7	0.2780	0.0003	0.0381	0.0001	0.0007	0.0000	1.6888	0.0004	0.0006	0.0000	2.5	0.2	43	4	0.1371	0.0004	0.0022	0.0001
F72	8	0.2192	0.0003	0.0305	0.0001	0.0005	0.0000	1.9506	0.0004	0.0003	0.0000	3.8	0.3	65	5	0.1393	0.0004	0.0016	0.0001
F73	1	0.0716	0.0002	0.0018	0.0000	0.0001	0.0000	0.0121	0.0004	0.0002	0.0000	1.5	2.8	25	96	0.0247	0.0005	0.0033	0.0002
F73	2	0.6515	0.0005	0.0178	0.0001	0.0006	0.0000	0.1463	0.0004	0.0020	0.0000	3.6	0.4	61	13	0.0273	0.0001	0.0031	0.0000
F73	3	0.5149	0.0004	0.0187	0.0001	0.0005	0.0000	0.2115	0.0004	0.0014	0.0000	4.9	0.5	83	17	0.0362	0.0002	0.0028	0.0001
F73	4	0.5271	0.0005	0.0342	0.0001	0.0007	0.0000	0.6207	0.0004	0.0014	0.0000	3.5	0.1	58	5	0.0649	0.0003	0.0026	0.0000
F73	5	0.4229	0.0007	0.0438	0.0001	0.0007	0.0000	1.2184	0.0004	0.0009	0.0000	3.5	0.2	59	6	0.1037	0.0003	0.0022	0.0001
F73	6	0.3347	0.0003	0.0370	0.0001	0.0008	0.0000	1.7905	0.0004	0.0008	0.0000	3.0	0.1	50	5	0.1105	0.0003	0.0023	0.0001
F73	7	0.3990	0.0003	0.0530	0.0001	0.0012	0.0000	2.8760	0.0004	0.0009	0.0000	2.4	0.1	40	5	0.1327	0.0003	0.0023	0.0001
F73	8	0.3248	0.0003	0.0448	0.0001	0.0009	0.0000	3.1097	0.0004	0.0008	0.0000	2.0	0.2	33	7	0.1378	0.0004	0.0025	0.0001

Sample	Step	^{40}Ar	±	^{39}Ar	±	^{38}Ar	±	^{37}Ar	±	^{36}Ar	±	$^{40}Ar^*/^{39}Ar$	±	Age	±	$^{39}Ar/^{40}Ar$	±	$^{36}Ar/^{40}Ar$	±
F74	1	0.0034	0.0001	0.0000	0.0000	0.0000	0.0000	0.0008	0.0003	0.0000	0.0000	-157.8	-285.8	NaN	9815	-0.0064	-0.0079	-0.0001	-0.0046
F74	2	0.4999	0.0006	0.0027	0.0000	0.0004	0.0000	0.1397	0.0003	0.0017	0.0000	3.1	1.7	52	29	0.0055	0.0001	0.0033	0.0000
F74	3	0.1079	0.0003	0.0023	0.0000	0.0000	0.0000	0.0985	0.0003	0.0003	0.0000	9.0	2.0	149	32	0.0216	0.0003	0.0027	0.0001
F74	4	0.2008	0.0004	0.0076	0.0000	0.0003	0.0000	0.3302	0.0003	0.0007	0.0000	0.7	0.6	11	11	0.0379	0.0002	0.0033	0.0001
F74	5	0.0857	0.0003	0.0058	0.0001	0.0001	0.0000	0.2583	0.0003	0.0002	0.0000	4.0	0.8	67	13	0.0681	0.0008	0.0025	0.0002
F74	6	0.0978	0.0002	0.0076	0.0001	0.0003	0.0000	0.5062	0.0003	0.0002	0.0000	3.7	0.6	62	10	0.0776	0.0006	0.0024	0.0002
F74	7	0.0839	0.0002	0.0066	0.0000	0.0003	0.0000	0.5374	0.0003	0.0002	0.0000	2.1	0.7	35	12	0.0784	0.0006	0.0028	0.0002
F74	8	0.0496	0.0002	0.0045	0.0000	0.0001	0.0000	0.4447	0.0003	0.0002	0.0000	1.0	1.0	17	18	0.0913	0.0010	0.0031	0.0003
F75	1	0.2969	0.0006	0.0036	0.0000	0.0002	0.0000	0.0384	0.0004	0.0010	0.0000	4.0	1.7	66	28	0.0122	0.0001	0.0032	0.0001
F75	2	1.0608	0.0010	0.0271	0.0001	0.0009	0.0000	0.2536	0.0004	0.0035	0.0000	1.2	0.3	20	6	0.0256	0.0001	0.0033	0.0000
F75	3	0.6281	0.0007	0.0336	0.0001	0.0007	0.0000	0.6711	0.0004	0.0018	0.0000	2.5	0.2	43	3	0.0535	0.0002	0.0029	0.0000
F75	4	0.5833	0.0005	0.0421	0.0002	0.0007	0.0000	1.3000	0.0004	0.0016	0.0000	2.3	0.2	39	4	0.0722	0.0004	0.0028	0.0001
F75	5	0.5310	0.0005	0.0458	0.0002	0.0008	0.0000	1.9540	0.0004	0.0014	0.0000	2.7	0.2	45	3	0.0863	0.0004	0.0026	0.0001
F75	6	0.9867	0.0012	0.0586	0.0001	0.0012	0.0000	3.3773	0.0009	0.0029	0.0001	2.3	0.3	38	5	0.0594	0.0002	0.0029	0.0001
F75	7	0.6266	0.0008	0.0394	0.0002	0.0008	0.0000	2.7733	0.0009	0.0019	0.0000	1.9	0.3	32	5	0.0629	0.0004	0.0030	0.0001
F75	8	0.2721	0.0006	0.0202	0.0001	0.0004	0.0000	1.7312	0.0009	0.0008	0.0000	2.3	0.4	38	7	0.0742	0.0004	0.0028	0.0001
F76	1	0.0173	0.0002	0.0001	0.0000	0.0000	0.0000	0.0019	0.0007	0.0001	0.0000	-33.3	-57.1	-687	1431	0.0073	0.0014	0.0042	0.0014
F76	2	0.3581	0.0004	0.0038	0.0000	0.0004	0.0000	0.0458	0.0007	0.0012	0.0000	3.9	2.3	66	38	0.0107	0.0001	0.0032	0.0001
F76	3	0.5566	0.0005	0.0153	0.0000	0.0006	0.0000	0.2511	0.0007	0.0019	0.0000	0.1	0.6	2	10	0.0275	0.0001	0.0034	0.0001
F76	4	0.5500	0.0006	0.0219	0.0001	0.0006	0.0000	0.6257	0.0007	0.0017	0.0000	2.1	0.4	35	7	0.0399	0.0002	0.0031	0.0001
F76	5	0.4839	0.0006	0.0251	0.0001	0.0007	0.0000	1.1285	0.0007	0.0015	0.0000	1.9	0.4	33	6	0.0519	0.0002	0.0030	0.0001
F76	6	0.5244	0.0004	0.0307	0.0001	0.0008	0.0000	1.6920	0.0007	0.0016	0.0000	2.1	0.2	36	4	0.0586	0.0002	0.0030	0.0000
F76	7	0.4487	0.0004	0.0297	0.0001	0.0008	0.0000	2.0013	0.0007	0.0012	0.0000	3.5	0.4	60	6	0.0661	0.0002	0.0026	0.0001
F76	8	0.2254	0.0003	0.0167	0.0001	0.0004	0.0000	1.2416	0.0007	0.0007	0.0000	1.6	0.5	27	9	0.0739	0.0003	0.0030	0.0001
F76	9	0.2126	0.0003	0.0172	0.0001	0.0005	0.0000	1.7171	0.0007	0.0006	0.0000	2.6	0.5	44	9	0.0810	0.0005	0.0027	0.0001

Sample	Step	^{40}Ar	±	^{39}Ar	±	^{38}Ar	±	^{37}Ar	±	^{36}Ar	±	$^{40}Ar^*/^{39}Ar$	±	Age	±	$^{39}Ar/^{40}Ar$	±	$^{36}Ar/^{40}Ar$	±
F77	1	0.2829	0.0003	0.0009	0.0000	0.0001	0.0000	0.0047	0.0008	0.0009	0.0000	21.5	8.0	335	114	0.0030	0.0002	0.0032	0.0001
F77	2	1.0163	0.0006	0.0098	0.0000	0.0009	0.0000	0.0594	0.0008	0.0034	0.0000	2.4	0.9	40	15	0.0097	0.0000	0.0033	0.0000
F77	3	0.7868	0.0019	0.0163	0.0001	0.0010	0.0000	0.2334	0.0008	0.0025	0.0000	2.3	0.5	39	9	0.0207	0.0001	0.0032	0.0000
F77	4	0.7549	0.0005	0.0185	0.0001	0.0008	0.0000	0.6512	0.0008	0.0024	0.0000	2.7	0.4	46	6	0.0245	0.0001	0.0032	0.0000
F77	5	0.4476	0.0005	0.0143	0.0000	0.0004	0.0000	0.8477	0.0002	0.0013	0.0000	3.7	0.6	62	9	0.0319	0.0001	0.0030	0.0001
F77	6	0.4525	0.0004	0.0124	0.0001	0.0005	0.0000	1.1107	0.0002	0.0015	0.0000	1.7	0.6	30	11	0.0274	0.0002	0.0032	0.0001
F77	7	0.5365	0.0004	0.0141	0.0001	0.0007	0.0000	1.6710	0.0002	0.0018	0.0000	1.2	0.7	20	12	0.0264	0.0001	0.0033	0.0001
F77	8	0.3045	0.0006	0.0099	0.0000	0.0006	0.0000	1.4457	0.0002	0.0010	0.0000	1.2	0.6	21	10	0.0327	0.0002	0.0032	0.0001

20.5 Ar/Ar age data for T5

Sample	Step	^{40}Ar	±	^{39}Ar	±	^{38}Ar	±	^{37}Ar	±	^{36}Ar	±	^{40}Ar*/^{39}Ar	±	Age	±	^{39}Ar/^{40}Ar	±	^{36}Ar/^{40}Ar	±
F79	1	0.0629	0.0004	0.0004	0.0000	0.0002	0.0001	0.0012	0.0001	0.0002	0.0000	-12.3	-30.1	-223	1158	0.0064	0.0003	0.0037	0.0007
F79	2	0.9812	0.0010	0.0091	0.0000	0.0008	0.0001	0.0692	0.0001	0.0033	0.0000	0.9	1.5	16	49	0.0093	0.0000	0.0034	0.0000
F79	3	0.6446	0.0011	0.0180	0.0001	0.0007	0.0000	0.1868	0.0004	0.0022	0.0000	-0.4	-0.3	-7	12	0.0280	0.0001	0.0034	0.0000
F79	4	0.6040	0.0006	0.0204	0.0001	0.0007	0.0000	0.4951	0.0004	0.0020	0.0000	0.5	0.6	9	22	0.0339	0.0001	0.0033	0.0001
F79	5	0.8158	0.0010	0.0309	0.0001	0.0011	0.0001	1.2238	0.0002	0.0025	0.0000	3.0	0.2	50	8	0.0379	0.0001	0.0030	0.0000
F79	6	0.4373	0.0004	0.0287	0.0001	0.0007	0.0000	1.4954	0.0003	0.0012	0.0000	3.2	0.1	54	5	0.0657	0.0003	0.0027	0.0000
F79	7	0.3088	0.0007	0.0203	0.0001	0.0006	0.0000	1.3061	0.0001	0.0009	0.0000	2.8	0.4	47	14	0.0658	0.0004	0.0028	0.0001
F79	8	0.3373	0.0008	0.0252	0.0002	0.0010	0.0000	2.2612	0.0004	0.0009	0.0000	2.4	0.4	40	14	0.0746	0.0005	0.0028	0.0001
F80	1	0.0177	0.0003	0.0006	0.0000	0.0000	0.0000	0.0039	0.0003	0.0001	0.0000	-11.3	-8.3	-206	318	0.0342	0.0017	0.0047	0.0010
F80	2	0.2319	0.0003	0.0087	0.0000	0.0002	0.0000	0.0706	0.0003	0.0008	0.0000	1.0	0.8	17	28	0.0374	0.0001	0.0033	0.0001
F80	3	0.3770	0.0007	0.0174	0.0001	0.0005	0.0000	0.1417	0.0003	0.0011	0.0000	3.2	0.4	54	14	0.0462	0.0002	0.0029	0.0001
F80	4	0.4149	0.0007	0.0299	0.0001	0.0007	0.0000	0.4136	0.0003	0.0013	0.0000	1.5	0.2	25	8	0.0721	0.0002	0.0030	0.0001
F80	5	0.4697	0.0009	0.0440	0.0001	0.0009	0.0000	1.0364	0.0005	0.0013	0.0000	1.8	0.2	31	5	0.0937	0.0002	0.0028	0.0000
F80	6	0.4402	0.0016	0.0427	0.0003	0.0007	0.0000	1.5013	0.0005	0.0011	0.0000	3.0	0.2	50	7	0.0971	0.0007	0.0024	0.0001
F80	7	0.3607	0.0005	0.0455	0.0001	0.0008	0.0000	2.0433	0.0006	0.0008	0.0000	2.9	0.2	48	5	0.1260	0.0002	0.0022	0.0001
F80	8	0.2052	0.0002	0.0244	0.0001	0.0005	0.0000	1.1107	0.0005	0.0004	0.0000	3.2	0.3	54	11	0.1189	0.0003	0.0021	0.0001
F80	9	0.3943	0.0005	0.0469	0.0002	0.0011	0.0000	2.6392	0.0005	0.0008	0.0000	3.4	0.2	57	6	0.1189	0.0004	0.0020	0.0001
F81	1	0.0089	0.0001	0.0003	0.0000	0.0001	0.0000	0.0035	0.0002	0.0000	0.0000	19.3	32.5	304	942	0.0307	0.0032	0.0014	0.0034
F81	2	0.1506	0.0003	0.0015	0.0000	0.0001	0.0000	0.0168	0.0002	0.0005	0.0000	8.2	7.0	136	222	0.0098	0.0002	0.0031	0.0002
F81	3	0.5045	0.0007	0.0221	0.0001	0.0006	0.0000	0.2354	0.0002	0.0017	0.0000	0.1	0.5	1	16	0.0438	0.0002	0.0034	0.0001
F81	4	0.3563	0.0010	0.0322	0.0001	0.0007	0.0000	0.4978	0.0002	0.0011	0.0000	1.0	0.3	18	9	0.0905	0.0004	0.0031	0.0001
F81	5	0.5920	0.0005	0.0548	0.0001	0.0015	0.0000	1.4513	0.0002	0.0017	0.0000	1.9	0.2	32	6	0.0926	0.0003	0.0028	0.0001
F81	6	0.6699	0.0004	0.0522	0.0001	0.0013	0.0000	2.1615	0.0000	0.0018	0.0000	2.4	0.2	40	5	0.0779	0.0002	0.0028	0.0000
F81	7	0.4532	0.0007	0.0351	0.0001	0.0009	0.0000	1.6643	0.0002	0.0012	0.0000	2.9	0.3	49	10	0.0774	0.0002	0.0026	0.0001
F81	8	0.7350	0.0011	0.0608	0.0001	0.0017	0.0000	3.5536	0.0002	0.0018	0.0000	3.1	0.1	53	5	0.0828	0.0002	0.0025	0.0000

Sample	Step	^{40}Ar	±	^{39}Ar	±	^{38}Ar	±	^{37}Ar	±	^{36}Ar	±	$^{40}Ar^*/^{39}Ar$	±	Age	±	$^{39}Ar/^{40}Ar$	±	$^{36}Ar/^{40}Ar$	±
F82	1	-0.0002	0.0005	0.0000	0.0000	0.0000	0.0000	-0.0006	0.0007	0.0000	0.0000	-292.0	-775.8	NaN	7510	0.0994	0.3304	0.1016	0.2857
F82	2	0.0879	0.0006	0.0047	0.0001	0.0001	0.0000	0.0612	0.0007	0.0002	0.0000	4.1	1.3	68	22	0.0529	0.0009	0.0027	0.0002
F82	3	0.2666	0.0007	0.0254	0.0001	0.0004	0.0000	0.4660	0.0007	0.0006	0.0000	3.1	0.3	52	5	0.0952	0.0006	0.0024	0.0001
F82	4	0.7356	0.0013	0.0703	0.0002	0.0010	0.0000	1.8948	0.0007	0.0018	0.0000	3.0	0.1	50	3	0.0956	0.0003	0.0024	0.0000
F82	5	0.4084	0.0013	0.0563	0.0001	0.0008	0.0000	1.5166	0.0007	0.0008	0.0000	3.2	0.2	53	3	0.1379	0.0005	0.0019	0.0001
F82	6	0.2888	0.0006	0.0456	0.0002	0.0007	0.0000	1.2918	0.0007	0.0005	0.0000	2.9	0.2	49	3	0.1580	0.0007	0.0018	0.0001
F82	7	0.3346	0.0010	0.0506	0.0003	0.0008	0.0000	1.9165	0.0007	0.0006	0.0000	2.9	0.2	48	3	0.1511	0.0011	0.0019	0.0001
F82	8	0.3661	0.0008	0.0547	0.0003	0.0009	0.0000	2.4715	0.0007	0.0008	0.0000	2.6	0.2	44	3	0.1495	0.0008	0.0021	0.0001
F82	9	0.2987	0.0007	0.0465	0.0002	0.0006	0.0000	2.5804	0.0007	0.0007	0.0000	2.3	0.1	38	2	0.1558	0.0008	0.0022	0.0001
F82	10	0.1308	0.0006	0.0192	0.0001	0.0003	0.0000	1.8410	0.0007	0.0004	0.0000	1.2	0.4	21	7	0.1468	0.0011	0.0028	0.0002
F83	1	0.0179	0.0003	0.0011	0.0001	0.0001	0.0000	0.0247	0.0004	0.0001	0.0000	1.4	7.4	24	125	0.0614	0.0031	0.0031	0.0015
F83	2	0.0594	0.0003	0.0052	0.0001	0.0001	0.0000	0.1252	0.0004	0.0001	0.0000	3.0	1.6	50	26	0.0875	0.0010	0.0025	0.0005
F83	3	0.1182	0.0003	0.0138	0.0001	0.0002	0.0000	0.4680	0.0004	0.0002	0.0000	3.5	0.6	59	10	0.1164	0.0007	0.0020	0.0002
F83	4	0.0938	0.0003	0.0154	0.0001	0.0003	0.0000	0.6109	0.0004	0.0002	0.0000	2.6	0.6	45	10	0.1640	0.0009	0.0019	0.0003
F83	5	0.1247	0.0003	0.0220	0.0001	0.0005	0.0000	1.1136	0.0004	0.0002	0.0000	2.6	0.4	44	6	0.1762	0.0008	0.0018	0.0002
F83	6	0.0850	0.0003	0.0156	0.0001	0.0003	0.0000	1.1389	0.0004	0.0002	0.0000	2.2	0.5	38	9	0.1832	0.0011	0.0020	0.0003
F83	7	0.0659	0.0003	0.0134	0.0001	0.0002	0.0000	1.1045	0.0004	0.0001	0.0000	2.7	0.7	46	12	0.2036	0.0017	0.0015	0.0005
F83	8	0.0429	0.0003	0.0081	0.0001	0.0002	0.0000	1.4196	0.0004	0.0001	0.0000	1.8	1.2	30	20	0.1898	0.0018	0.0022	0.0008
F84	1	0.0043	0.0005	0.0001	0.0000	0.0000	0.0000	0.0042	0.0009	0.0000	0.0000	-19.9	-54.4	-378	1151	0.0312	0.0076	0.0055	0.0057
F84	2	0.1237	0.0005	0.0089	0.0001	0.0002	0.0000	0.1593	0.0009	0.0004	0.0000	1.9	0.8	32	14	0.0720	0.0007	0.0029	0.0002
F84	3	0.1842	0.0005	0.0262	0.0001	0.0003	0.0000	0.4070	0.0009	0.0004	0.0000	2.1	0.3	36	6	0.1425	0.0009	0.0024	0.0002
F84	4	0.3752	0.0005	0.0540	0.0001	0.0008	0.0000	1.2087	0.0009	0.0008	0.0000	2.3	0.2	40	3	0.1439	0.0003	0.0022	0.0001
F84	5	0.3554	0.0006	0.0467	0.0001	0.0007	0.0000	1.4333	0.0009	0.0008	0.0000	2.7	0.2	46	3	0.1315	0.0005	0.0022	0.0001
F84	6	0.5180	0.0013	0.0690	0.0001	0.0013	0.0000	3.6126	0.0009	0.0011	0.0000	2.7	0.2	45	3	0.1331	0.0004	0.0022	0.0001
F84	7	0.2842	0.0006	0.0379	0.0001	0.0007	0.0000	2.8606	0.0009	0.0007	0.0000	2.0	0.2	34	4	0.1335	0.0005	0.0025	0.0001
F84	8	0.1674	0.0005	0.0164	0.0001	0.0003	0.0000	2.8303	0.0009	0.0006	0.0000	-0.5	-0.7	-9	12	0.0979	0.0006	0.0036	0.0002

Sample	Step	^{40}Ar	±	^{39}Ar	±	^{38}Ar	±	^{37}Ar	±	^{36}Ar	±	$^{40}Ar^*/^{39}Ar$	±	Age	±	$^{39}Ar/^{40}Ar$	±	$^{36}Ar/^{40}Ar$	±
F85	1	0.0585	0.0003	0.0005	0.0001	0.0001	0.0001	0.0074	0.0008	0.0002	0.0000	4.6	21.5	78	355	0.0091	0.0011	0.0032	0.0007
F85	2	0.3351	0.0004	0.0079	0.0001	0.0004	0.0001	0.0896	0.0008	0.0012	0.0000	-2.8	-1.6	-49	28	0.0235	0.0002	0.0036	0.0001
F85	3	0.3009	0.0006	0.0134	0.0001	0.0004	0.0001	0.2679	0.0008	0.0010	0.0000	1.5	0.9	26	16	0.0446	0.0003	0.0032	0.0001
F85	4	0.4210	0.0004	0.0348	0.0001	0.0009	0.0001	1.1095	0.0008	0.0010	0.0000	3.8	0.3	65	5	0.0826	0.0003	0.0023	0.0001
F85	5	0.6647	0.0006	0.0589	0.0001	0.0014	0.0001	1.9480	0.0008	0.0016	0.0000	3.2	0.2	55	4	0.0886	0.0002	0.0024	0.0001
F85	6	0.5578	0.0005	0.0486	0.0001	0.0012	0.0001	1.6397	0.0008	0.0013	0.0000	3.5	0.3	59	4	0.0871	0.0003	0.0024	0.0001
F85	7	0.3366	0.0003	0.0289	0.0001	0.0008	0.0001	1.2102	0.0008	0.0009	0.0000	2.3	0.4	40	7	0.0858	0.0003	0.0027	0.0001
F85	8	0.5917	0.0003	0.0431	0.0001	0.0011	0.0001	2.2452	0.0008	0.0015	0.0000	3.5	0.3	60	5	0.0728	0.0002	0.0025	0.0001
F86	1	0.0603	0.0004	0.0033	0.0000	0.0001	0.0000	0.0576	0.0003	0.0002	0.0000	1.8	1.3	31	22	0.0546	0.0008	0.0030	0.0002
F86	2	0.1515	0.0004	0.0199	0.0001	0.0002	0.0000	0.4860	0.0003	0.0003	0.0000	2.7	0.2	46	4	0.1310	0.0007	0.0022	0.0001
F86	3	0.2356	0.0006	0.0353	0.0002	0.0004	0.0000	1.1698	0.0003	0.0005	0.0000	2.6	0.2	44	3	0.1500	0.0009	0.0021	0.0001
F86	4	0.3374	0.0006	0.0464	0.0002	0.0006	0.0000	1.7987	0.0003	0.0007	0.0000	2.9	0.1	50	2	0.1376	0.0006	0.0020	0.0000
F86	5	0.2342	0.0006	0.0253	0.0001	0.0004	0.0000	1.3220	0.0003	0.0006	0.0000	2.6	0.3	44	4	0.1080	0.0005	0.0024	0.0001
F86	6	0.3970	0.0008	0.0306	0.0001	0.0007	0.0000	2.3952	0.0003	0.0011	0.0000	2.3	0.2	39	4	0.0770	0.0004	0.0028	0.0001
F86	7	0.2809	0.0007	0.0204	0.0002	0.0005	0.0000	3.3413	0.0003	0.0009	0.0000	0.5	0.2	9	4	0.0728	0.0006	0.0033	0.0001
F86	8	0.1648	0.0005	0.0136	0.0001	0.0003	0.0000	1.9438	0.0003	0.0005	0.0000	0.7	0.5	13	8	0.0825	0.0008	0.0032	0.0001
F87	1	0.0486	0.0006	0.0026	0.0000	0.0000	0.0000	0.0273	0.0005	0.0002	0.0000	1.5	3.1	25	53	0.0525	0.0009	0.0031	0.0006
F87	2	0.2476	0.0007	0.0192	0.0001	0.0003	0.0000	0.3464	0.0005	0.0007	0.0000	1.4	0.3	24	5	0.0776	0.0006	0.0030	0.0001
F87	3	0.1931	0.0006	0.0203	0.0001	0.0003	0.0000	0.6107	0.0005	0.0005	0.0000	2.1	0.4	36	7	0.1051	0.0006	0.0026	0.0001
F87	4	0.2568	0.0007	0.0317	0.0001	0.0005	0.0000	1.4077	0.0005	0.0006	0.0000	2.2	0.3	37	4	0.1235	0.0005	0.0025	0.0001
F87	5	0.1842	0.0007	0.0243	0.0001	0.0004	0.0000	1.4051	0.0005	0.0004	0.0000	2.1	0.3	37	6	0.1320	0.0008	0.0024	0.0001
F87	6	0.2836	0.0008	0.0304	0.0001	0.0007	0.0000	3.0221	0.0005	0.0009	0.0000	0.8	0.3	14	5	0.1071	0.0005	0.0031	0.0001
F87	7	0.1443	0.0006	0.0145	0.0001	0.0004	0.0000	2.3471	0.0005	0.0005	0.0000	0.0	0.7	1	12	0.1001	0.0006	0.0034	0.0002
F87	8	0.0829	0.0004	0.0069	0.0001	0.0001	0.0000	1.6704	0.0004	0.0003	0.0000	-1.4	-0.9	-25	16	0.0833	0.0010	0.0038	0.0003

20.6 Ar/Ar age data for T6

Sample	Step	^{40}Ar	±	^{39}Ar	±	^{38}Ar	±	^{37}Ar	±	^{36}Ar	±	^{40}Ar*/^{39}Ar	±	Age	±	^{39}Ar/^{40}Ar	±	^{36}Ar/^{40}Ar	±
F59	1	0.1143	0.0003	0.0031	0.0001	0.0000	0.0001	0.0217	0.0004	0.0004	0.0000	-0.34	-2.55	-6	44	0.0274	0.0007	0.0034	0.0002
F59	2	0.3554	0.0006	0.0079	0.0001	0.0003	0.0001	0.0809	0.0004	0.0012	0.0000	-0.82	-1.46	-14	25	0.0222	0.0002	0.0034	0.0001
F59	3	0.9030	0.0006	0.0144	0.0001	0.0006	0.0001	0.2158	0.0004	0.0030	0.0000	1.58	0.66	27	11	0.0160	0.0001	0.0033	0.0000
F59	4	1.8078	0.0039	0.0172	0.0001	0.0014	0.0001	0.7195	0.0004	0.0059	0.0000	3.13	0.59	53	10	0.0095	0.0001	0.0033	0.0000
F59	5	2.2347	0.0009	0.0144	0.0001	0.0017	0.0001	1.2832	0.0004	0.0075	0.0000	0.95	0.80	16	14	0.0064	0.0000	0.0034	0.0000
F59	6	1.8738	0.0013	0.0095	0.0001	0.0014	0.0001	1.1513	0.0004	0.0062	0.0000	3.75	0.85	63	14	0.0051	0.0000	0.0033	0.0000
F59	7	1.0153	0.0011	0.0045	0.0001	0.0008	0.0001	0.6517	0.0004	0.0035	0.0000	-4.46	-1.80	-78	32	0.0044	0.0001	0.0035	0.0000
F59	8	1.9072	0.0035	0.0090	0.0001	0.0014	0.0001	2.7166	0.0004	0.0065	0.0000	-0.40	-1.13	-7	19	0.0047	0.0000	0.0034	0.0000
F60	1	0.0196	0.0008	0.0002	0.0001	0.0000	0.0001	0.0039	0.0035	0.0000	0.0000	70.78	55.12	928	565	0.0112	0.0043	0.0007	0.0018
F60	2	0.1761	0.0009	0.0034	0.0001	0.0002	0.0001	0.0945	0.0035	0.0005	0.0000	7.43	3.09	123	49	0.0194	0.0005	0.0029	0.0002
F60	3	0.6249	0.0008	0.0116	0.0001	0.0006	0.0001	0.4030	0.0035	0.0019	0.0000	4.24	1.01	71	17	0.0186	0.0001	0.0031	0.0001
F60	4	1.0545	0.0009	0.0121	0.0001	0.0008	0.0001	0.5880	0.0035	0.0034	0.0000	2.92	0.97	49	16	0.0115	0.0001	0.0033	0.0000
F60	5	2.1552	0.0014	0.0155	0.0001	0.0017	0.0001	1.7076	0.0035	0.0072	0.0001	1.73	1.01	29	17	0.0072	0.0000	0.0033	0.0000
F60	6	1.9748	0.0023	0.0143	0.0001	0.0018	0.0001	1.9850	0.0035	0.0069	0.0001	-4.46	-1.61	-78	29	0.0073	0.0001	0.0035	0.0000
F60	7	1.1593	0.0012	0.0099	0.0001	0.0012	0.0001	2.0001	0.0035	0.0042	0.0000	-7.24	-1.37	-129	25	0.0085	0.0001	0.0036	0.0000
F60	8	1.0717	0.0013	0.0096	0.0001	0.0011	0.0001	2.9087	0.0035	0.0038	0.0000	-5.14	-1.23	-90	22	0.0090	0.0001	0.0035	0.0000
F61	1	0.0218	0.0003	0.0007	0.0001	0.0001	0.0001	0.0117	0.0002	0.0000	0.0000	26.75	14.03	409	192	0.0322	0.0024	0.0005	0.0015
F61	2	0.1527	0.0003	0.0073	0.0001	0.0002	0.0001	0.0973	0.0002	0.0005	0.0000	-0.03	-1.51	-1	26	0.0478	0.0004	0.0034	0.0002
F61	3	0.4135	0.0004	0.0211	0.0001	0.0006	0.0001	0.4048	0.0002	0.0013	0.0000	1.03	0.46	18	8	0.0510	0.0002	0.0032	0.0001
F61	4	0.6864	0.0017	0.0299	0.0001	0.0008	0.0001	1.0314	0.0002	0.0021	0.0000	2.40	0.48	41	8	0.0435	0.0002	0.0030	0.0001
F61	5	0.5645	0.0007	0.0227	0.0001	0.0007	0.0001	1.3924	0.0002	0.0016	0.0000	3.73	0.55	63	9	0.0402	0.0001	0.0029	0.0001
F61	6	0.4199	0.0004	0.0145	0.0001	0.0005	0.0001	1.5885	0.0002	0.0014	0.0000	-0.23	-0.86	-4	15	0.0345	0.0002	0.0034	0.0001
F61	7	0.5000	0.0023	0.0151	0.0000	0.0006	0.0000	2.3871	0.0018	0.0017	0.0000	0.26	0.62	5	11	0.0302	0.0002	0.0034	0.0001
F61	8	0.3471	0.0006	0.0134	0.0000	0.0005	0.0000	3.0292	0.0018	0.0011	0.0000	1.02	0.68	17	12	0.0387	0.0001	0.0033	0.0001

Sample	Step	^{40}Ar	±	^{39}Ar	±	^{38}Ar	±	^{37}Ar	±	^{36}Ar	±	$^{40}Ar^*/^{39}Ar$	±	Age	±	$^{39}Ar/^{40}Ar$	±	$^{36}Ar/^{40}Ar$	±
F62	2	0.3494	0.0002	0.0025	0.0001	0.0003	0.0001	0.0329	0.0006	0.0011	0.0000	15.49	3.48	248	52	0.0071	0.0003	0.0030	0.0001
F62	3	0.5803	0.0003	0.0107	0.0001	0.0005	0.0001	0.1346	0.0006	0.0019	0.0000	1.87	0.63	32	11	0.0184	0.0002	0.0033	0.0000
F62	4	0.2483	0.0002	0.0191	0.0001	0.0003	0.0001	0.2758	0.0006	0.0007	0.0000	2.66	0.35	45	6	0.0768	0.0005	0.0027	0.0001
F62	5	0.2738	0.0003	0.0313	0.0001	0.0005	0.0001	0.6644	0.0006	0.0006	0.0000	2.65	0.27	45	5	0.1144	0.0005	0.0024	0.0001
F62	6	0.2311	0.0004	0.0323	0.0001	0.0005	0.0001	0.9620	0.0006	0.0004	0.0000	3.16	0.21	54	4	0.1396	0.0007	0.0019	0.0001
F62	7	0.2157	0.0003	0.0407	0.0001	0.0008	0.0001	1.2019	0.0006	0.0003	0.0000	3.02	0.17	51	3	0.1888	0.0007	0.0015	0.0001
F62	8	0.2341	0.0002	0.0451	0.0001	0.0008	0.0001	1.4569	0.0006	0.0005	0.0000	2.01	0.19	34	3	0.1924	0.0006	0.0021	0.0001
F62	9	0.1918	0.0003	0.0388	0.0001	0.0006	0.0001	1.6810	0.0006	0.0003	0.0000	2.30	0.17	39	3	0.2024	0.0006	0.0018	0.0001
F63	1	0.0437	0.0005	0.0006	0.0001	0.0001	0.0000	0.0050	0.0012	0.0001	0.0000	9.46	21.68	156	342	0.0138	0.0012	0.0029	0.0010
F63	2	0.6027	0.0016	0.0095	0.0001	0.0005	0.0000	0.0687	0.0012	0.0019	0.0001	3.37	1.65	57	28	0.0157	0.0001	0.0032	0.0001
F63	3	1.0885	0.0013	0.0308	0.0001	0.0010	0.0000	0.2757	0.0012	0.0035	0.0000	2.23	0.23	38	4	0.0283	0.0001	0.0032	0.0000
F63	4	1.3190	0.0008	0.0473	0.0003	0.0017	0.0000	0.8997	0.0012	0.0041	0.0000	2.17	0.19	37	3	0.0358	0.0002	0.0031	0.0000
F63	5	2.1250	0.0031	0.0822	0.0001	0.0022	0.0000	2.4620	0.0012	0.0062	0.0000	3.45	0.11	58	2	0.0387	0.0001	0.0029	0.0000
F63	6	0.9699	0.0009	0.0674	0.0001	0.0015	0.0000	2.6061	0.0012	0.0025	0.0000	3.37	0.16	57	3	0.0695	0.0002	0.0026	0.0000
F63	7	1.2127	0.0012	0.0941	0.0001	0.0021	0.0000	3.8387	0.0012	0.0030	0.0000	3.44	0.10	58	2	0.0776	0.0001	0.0025	0.0000
F63	8	0.7282	0.0015	0.0766	0.0001	0.0014	0.0000	3.3974	0.0012	0.0017	0.0000	2.93	0.15	50	2	0.1052	0.0003	0.0023	0.0001
F64	1	0.7736	0.0005	0.0400	0.0001	0.0007	0.0000	0.0556	0.0001	0.0014	0.0000	8.77	0.13	145	2	0.0517	0.0001	0.0019	0.0000
F64	2	1.0527	0.0011	0.0863	0.0002	0.0012	0.0001	0.2629	0.0001	0.0018	0.0000	5.91	0.06	99	1	0.0819	0.0002	0.0017	0.0000
F64	3	0.5071	0.0005	0.0844	0.0001	0.0012	0.0001	0.4668	0.0001	0.0007	0.0000	3.73	0.06	63	1	0.1664	0.0002	0.0013	0.0000
F64	4	0.4044	0.0004	0.1207	0.0001	0.0018	0.0001	1.2655	0.0001	0.0004	0.0000	2.47	0.04	42	1	0.2986	0.0005	0.0009	0.0000
F64	5	0.2679	0.0004	0.0936	0.0002	0.0014	0.0001	1.5700	0.0001	0.0001	0.0000	2.55	0.08	43	1	0.3493	0.0009	0.0004	0.0001
F64	6	0.2667	0.0005	0.0971	0.0003	0.0016	0.0001	1.8425	0.0001	0.0001	0.0000	2.42	0.05	41	1	0.3641	0.0013	0.0004	0.0001
F64	7	0.1442	0.0003	0.0574	0.0001	0.0008	0.0001	1.4307	0.0001	0.0000	0.0000	2.53	0.09	43	1	0.3980	0.0012	0.0000	-0.0001
F64	8	0.4360	0.0005	0.1753	0.0002	0.0028	0.0001	4.2000	0.0001	0.0001	0.0000	2.26	0.04	39	1	0.4019	0.0006	0.0003	0.0001

Sample	Step	^{40}Ar	±	^{39}Ar	±	^{38}Ar	±	^{37}Ar	±	^{36}Ar	±	$^{40}Ar^*/^{39}Ar$	±	Age	±	$^{39}Ar/^{40}Ar$	±	$^{36}Ar/^{40}Ar$	±
F65	1	0.2847	0.0002	0.0049	0.0001	0.0002	0.0000	0.0381	0.0015	0.0010	0.0000	-0.51	-2.19	-9	38	0.0172	0.0002	0.0034	0.0001
F65	2	0.6149	0.0009	0.0238	0.0001	0.0006	0.0000	0.2626	0.0015	0.0019	0.0000	2.34	0.50	40	8	0.0386	0.0002	0.0031	0.0001
F65	3	0.5327	0.0015	0.0323	0.0002	0.0009	0.0000	0.7586	0.0015	0.0016	0.0000	2.30	0.37	39	6	0.0606	0.0004	0.0029	0.0001
F65	4	0.5957	0.0006	0.0347	0.0001	0.0008	0.0000	1.0758	0.0015	0.0017	0.0000	2.80	0.31	48	5	0.0582	0.0001	0.0028	0.0001
F65	5	0.6239	0.0007	0.0433	0.0001	0.0012	0.0000	2.0302	0.0015	0.0017	0.0000	2.92	0.25	50	4	0.0693	0.0002	0.0027	0.0001
F65	6	0.3993	0.0014	0.0359	0.0001	0.0008	0.0000	2.1183	0.0015	0.0010	0.0000	3.22	0.30	55	5	0.0899	0.0004	0.0024	0.0001
F65	7	0.2584	0.0013	0.0255	0.0001	0.0005	0.0000	1.8970	0.0015	0.0006	0.0000	3.53	0.47	60	8	0.0989	0.0005	0.0022	0.0002
F65	8	0.3350	0.0003	0.0332	0.0001	0.0006	0.0001	2.9108	0.0015	0.0009	0.0000	1.81	0.36	31	6	0.0991	0.0002	0.0028	0.0001
F67	1	0.2726	0.0004	0.0046	0.0000	0.0002	0.0000	0.0366	0.0018	0.0009	0.0000	1.80	2.20	31	37	0.0168	0.0002	0.2726	0.0004
F67	2	0.5382	0.0009	0.0111	0.0001	0.0004	0.0000	0.1494	0.0018	0.0018	0.0000	0.97	0.91	17	16	0.0205	0.0002	0.5382	0.0009
F67	3	0.6383	0.0006	0.0223	0.0001	0.0006	0.0000	0.4997	0.0018	0.0021	0.0000	1.04	0.45	18	8	0.0349	0.0001	0.6383	0.0006
F67	4	1.1208	0.0010	0.0540	0.0002	0.0013	0.0001	1.4593	0.0018	0.0033	0.0000	2.60	0.19	44	3	0.0482	0.0002	1.1208	0.0010
F67	5	0.5554	0.0009	0.0414	0.0002	0.0010	0.0000	1.6461	0.0018	0.0015	0.0000	2.93	0.24	50	4	0.0746	0.0004	0.5554	0.0009
F67	6	0.3351	0.0006	0.0281	0.0001	0.0007	0.0000	1.7441	0.0018	0.0009	0.0000	2.02	0.31	35	5	0.0838	0.0003	0.3351	0.0006
F67	7	0.1806	0.0004	0.0155	0.0001	0.0005	0.0000	1.4024	0.0018	0.0005	0.0000	1.50	0.65	26	11	0.0858	0.0004	0.1806	0.0004
F67	8	0.2161	0.0003	0.0230	0.0001	0.0005	0.0000	2.5094	0.0018	0.0005	0.0000	2.46	0.44	42	7	0.1065	0.0004	0.2161	0.0003
F68	1	0.1483	0.0004	0.0029	0.0001	0.0002	0.0000	0.0305	0.0005	0.0004	0.0000	6.79	2.85	114	46	0.0193	0.0004	0.0029	0.0002
F68	2	0.1568	0.0005	0.0076	0.0001	0.0002	0.0000	0.1540	0.0005	0.0004	0.0000	4.55	1.07	77	18	0.0487	0.0004	0.0026	0.0002
F68	3	0.1243	0.0003	0.0093	0.0001	0.0003	0.0000	0.2913	0.0005	0.0003	0.0000	2.34	0.88	40	15	0.0749	0.0008	0.0028	0.0002
F68	4	0.0964	0.0003	0.0116	0.0001	0.0002	0.0000	0.5487	0.0005	0.0002	0.0000	2.24	0.83	38	14	0.1202	0.0008	0.0025	0.0003
F68	5	0.0642	0.0003	0.0096	0.0001	0.0002	0.0000	0.6145	0.0005	0.0001	0.0000	2.97	0.85	51	14	0.1489	0.0012	0.0019	0.0004
F68	6	0.0633	0.0003	0.0098	0.0001	0.0002	0.0000	0.8942	0.0005	0.0001	0.0000	2.34	0.84	40	14	0.1543	0.0014	0.0022	0.0004
F68	7	0.0367	0.0002	0.0052	0.0001	0.0002	0.0000	0.6140	0.0005	0.0001	0.0000	0.74	1.59	13	27	0.1405	0.0020	0.0030	0.0008
F68	8	0.0479	0.0003	0.0076	0.0001	0.0002	0.0000	0.7197	0.0005	0.0002	0.0000	-0.43	-1.08	-7	19	0.1579	0.0015	0.0036	0.0006

20.7 Ar/Ar age data for T7

Sample	Step	^{40}Ar	±	^{39}Ar	±	^{38}Ar	±	^{37}Ar	±	^{36}Ar	±	^{40}Ar*/^{39}Ar	±	Age	±	^{39}Ar/^{40}Ar	±	^{36}Ar/^{40}Ar	±
		0.5384	0.0008	0.0095	0.0001	0.0003	0.0000	0.1152	0.0001	0.0016	0.0000	5.36	0.70	90	23	0.0177	0.0001	0.0031	0.0000
		0.1227	0.0004	0.0092	0.0001	0.0001	0.0000	0.1322	0.0001	0.0003	0.0000	3.88	0.72	66	24	0.0746	0.0005	0.0024	0.0002
		0.1675	0.0007	0.0218	0.0001	0.0003	0.0000	0.3930	0.0001	0.0003	0.0000	3.53	0.31	60	10	0.1303	0.0010	0.0018	0.0001
		0.1278	0.0005	0.0242	0.0001	0.0003	0.0000	0.5814	0.0001	0.0002	0.0000	3.26	0.13	56	4	0.1891	0.0011	0.0013	0.0001
		0.1111	0.0003	0.0224	0.0001	0.0003	0.0000	0.7891	0.0001	0.0002	0.0000	2.97	0.13	51	5	0.2016	0.0014	0.0014	0.0001
		0.0805	0.0004	0.0146	0.0001	0.0002	0.0000	0.6010	0.0001	0.0002	0.0000	2.26	0.41	39	14	0.1814	0.0013	0.0020	0.0002
		0.0479	0.0005	0.0097	0.0001	0.0001	0.0000	0.4966	0.0001	0.0001	0.0000	2.25	0.87	39	29	0.2019	0.0024	0.0018	0.0006
		0.0063	0.0001	0.0000	0.0000	0.0000	0.0000	0.0009	0.0003	0.0000	0.0000	738.58	537.08	3762	1149	0.0026	0.0018	-0.0032	-0.0016
		0.0439	0.0002	0.0002	0.0000	0.0000	0.0000	0.0044	0.0003	0.0001	0.0000	37.98	25.78	558	326	0.0053	0.0005	0.0027	0.0005
		0.3959	0.0007	0.0107	0.0001	0.0003	0.0000	0.1469	0.0003	0.0011	0.0000	6.58	0.56	110	9	0.0271	0.0002	0.0028	0.0001
		0.4571	0.0007	0.0359	0.0002	0.0005	0.0000	0.7966	0.0003	0.0011	0.0000	3.77	0.17	64	3	0.0786	0.0005	0.0024	0.0000
		0.3034	0.0004	0.0351	0.0001	0.0006	0.0000	1.2687	0.0003	0.0007	0.0000	2.97	0.17	50	3	0.1157	0.0004	0.0022	0.0001
		0.0854	0.0003	0.0128	0.0001	0.0002	0.0000	0.6549	0.0003	0.0002	0.0000	2.59	0.46	44	8	0.1504	0.0015	0.0021	0.0002
		0.0361	0.0003	0.0053	0.0001	0.0001	0.0000	0.3925	0.0003	0.0001	0.0000	3.13	0.56	52	9	0.1467	0.0018	0.0018	0.0003
		0.0591	0.0004	0.0091	0.0001	0.0001	0.0000	0.9716	0.0003	0.0001	0.0000	2.51	0.33	43	6	0.1543	0.0016	0.0021	0.0002
		0.1814	0.0005	0.0253	0.0001	0.0003	0.0000	0.0060	0.0001	0.0003	0.0000	3.68	0.25	62	4	0.1396	0.0006	0.0016	0.0001
		0.2282	0.0004	0.0190	0.0001	0.0002	0.0000	0.0596	0.0001	0.0005	0.0000	3.85	0.43	65	7	0.0834	0.0006	0.0023	0.0001
		0.1857	0.0004	0.0269	0.0001	0.0003	0.0000	0.2474	0.0001	0.0003	0.0000	3.23	0.30	55	5	0.1449	0.0008	0.0018	0.0001
		0.1210	0.0003	0.0231	0.0001	0.0003	0.0000	0.5643	0.0001	0.0002	0.0000	2.94	0.35	50	6	0.1905	0.0012	0.0015	0.0002
		0.0622	0.0004	0.0120	0.0001	0.0002	0.0000	0.4686	0.0001	0.0001	0.0000	2.82	0.68	48	11	0.1929	0.0018	0.0015	0.0004
		0.0414	0.0003	0.0082	0.0001	0.0001	0.0000	0.3969	0.0001	0.0001	0.0000	2.70	0.98	46	16	0.1990	0.0022	0.0016	0.0007

Sample	Step	^{40}Ar	±	^{39}Ar	±	^{38}Ar	±	^{37}Ar	±	^{36}Ar	±	$^{40}Ar^*/^{39}Ar$	±	Age	±	$^{39}Ar/^{40}Ar$	±	$^{36}Ar/^{40}Ar$	±
		0.0004	0.0002	0.0001	0.0000	0.0000	0.0000	0.0002	0.0003	0.0000	0.0000	81.70	58.60	1032	1128	0.1649	0.0884	-0.0422	-0.0323
		0.4703	0.0007	0.0540	0.0002	0.0005	0.0000	0.0739	0.0003	0.0007	0.0000	4.97	0.11	83	4	0.1148	0.0004	0.0015	0.0000
		0.3975	0.0007	0.0841	0.0003	0.0008	0.0000	0.1534	0.0003	0.0003	0.0000	3.63	0.07	61	3	0.2117	0.0008	0.0008	0.0001
		0.6154	0.0009	0.1498	0.0003	0.0016	0.0000	0.6110	0.0003	0.0005	0.0000	3.10	0.02	52	1	0.2435	0.0006	0.0008	0.0000
		0.4078	0.0006	0.1084	0.0002	0.0011	0.0000	0.5902	0.0000	0.0003	0.0000	3.04	0.04	51	1	0.2659	0.0006	0.0006	0.0000
		0.1254	0.0005	0.0338	0.0002	0.0003	0.0000	0.2808	0.0000	0.0001	0.0000	2.70	0.13	45	4	0.2694	0.0016	0.0009	0.0001
		0.0706	0.0004	0.0177	0.0001	0.0002	0.0000	0.2352	0.0000	0.0001	0.0000	2.52	0.24	43	8	0.2510	0.0021	0.0012	0.0002